1974

Linear Stability Analysis Of A Class Of Solutions Of The Filament Model For A Stationary Field Electron Ring Accelerator

Techien Joseph Chen

LINEAR STABILITY ANALYSIS OF A CLASS OF SOLUTIONS OF THE FILAMENT MODEL FOR A STATIONARY FIELD ELECTRON RING ACCELERATOR

by

Techien Joseph Chen

Department of Applied Mathematics

Submitted in partial fulfillment

of the requirements for the degree of

Doctor of Philosophy

Faculty of Graduate Studies

The University of Western Ontario

London, Canada

August 1974

ABSTRACT

The stability of two of the short time scale solutions obtained in the filament model for a stationary field electron ring accelerator is studied by means of a linearized perturbation on the electron and ion distribution functions. The Vlasov equations for the electrons and ions are coupled. The coupling of these equations results in a Fredholm integral equation which can be converted into an infinite system of linear equations. A stability criterion is then obtained from the zeros of the truncated determinants of the coefficients of the infinite system. One of the equilibrium solutions, characterized by the dimensionless parameter $\varepsilon=0$, is entirely stable. The other solution, characterized by $\varepsilon>0$, is stable provided that both ε and the ratio of the square of the ion period to that of the electrons are not too large.

ACKNOWLEDGEMENTS

I wish to express my appreciation to Professor J.B. Ehrman for suggesting the problem considered in this thesis and for his aid and guidance in its preparation. Thanks are due to the Department of Applied Mathematics for providing the facilities to carry out this investigation and to the Computing Centre for providing the computing facilities. Finally, I wish to thank my wife for her support and for checking the equations.

TABLE OF CONTENTS

LIST OF TABLES

LIST OF FIGURES

1. Introduction.

The electron ring accelerator (ERA) is one of the many newly proposed ideas of accelerating protons or other heavy ions. Its basic difference from the conventional accelerators is in the driving and the guiding fields on the particles being accelerated. In the latter, these fields are provided for from some external sources; whereas, in an ERA a large part of these fields are provided by the particles themselves.

The underlying principle in an ERA is to form a stable nonneutral cluster of electrons and positive ions, with the number of ions being much less than that of the electrons. In such a cluster the electrons provide most of the charge, while the ions provide most of the mass, so that the gain in energy from the external fields by the ions is much higher than if the ions alone were being accelerated. This is one of two basic advantages of an ERA has over the conventional accelerators. A second advantage follows from the fact that the effective density and current of the cluster are no longer zero. This lifts the requirement of curl $\underline{E} = 0$, and div $\underline{E} = 0$ from Maxwell's equations, with the consequence of widening the variety of external acceleration fields, and providing an 'ultra-strong-focusing' for the cluster.

Although the advantages are great, this theoretical conjecture also has many difficulties. One obvious difficulty is the possible unstable nature of the non-neutral cluster. For example, a spherical 'blob' of electrons and ions, is known to be unstable. In the 1956 CERN Symposium on High Energy Accelerators at Geneva, Budker[1] proposed to stabilize the cluster by forming a ring of electrons circulating at relativistic speeds. The mutual repulsions between the electrons are reduced by a factor of γ^{-2}, where γ is the relativistic factor. He believed that with the introduction of a small fraction of positive ions, the residual repulsion can not only be overcome, but also resulted in a net overall attraction stabilizing the electron ring.

Early in the 1950's several authors[2-4] suggested the possibility of incorporating the self-fields into the accelerating mechanism. A more widespread interest in unconventional accelerators arose after the above mentioned Symposium. At this meeting two important papers were presented: 'Relativistic Stabilized electron Beam' by Budker,[1] in which the field associated with an intense relativistic electron ring was suggested as a possible high intensity guide field; and 'Coherent Principles of Acceleration of Charged Particles' by Veksler,[5] in which the coherent principle was first described and three methods of acceleration were suggested.

In the years immediately following this meeting, a number of physicists in the Soviet Union, Europe, and this Continent explored these possibilities in some detail. Among others: Levin, Askaryan, Rabinovish[6,7] investigated the rf acceleration as suggested by Veksler; de-Packh[8,9] modified Budker's design, and his modification was further studied by Godlove and dePackh,[10] and Ehrman.[11-13]

Meanwhile, Veksler and his group at Dubna continued on the feasibility studies of the ERA (of in their terminology, the collective linear ion accelerator). Their report[14] in September, 1967 at the International Conference on Accelerators, Cambridge, Mass., was received with enthusiasm. Their experiments were immediately put to test by many accelerator groups. The Lawrence Radiation Laboratory at Berkeley, the birth place of the cyclotron, has one of the most active group in testing the new ERA concept.[15]

These early efforts dealt mainly with the problem of ring formation. One of the methods used in Dubna[14] and Berkeley[15] was compression of an electron ring with a large radius by pulsed magnetic field into that of a small one. In this method, a large ring of electrons with radius of the order of 20 cm is formed by injecting electrons into an axisymmetric magnetic field in a direction at right

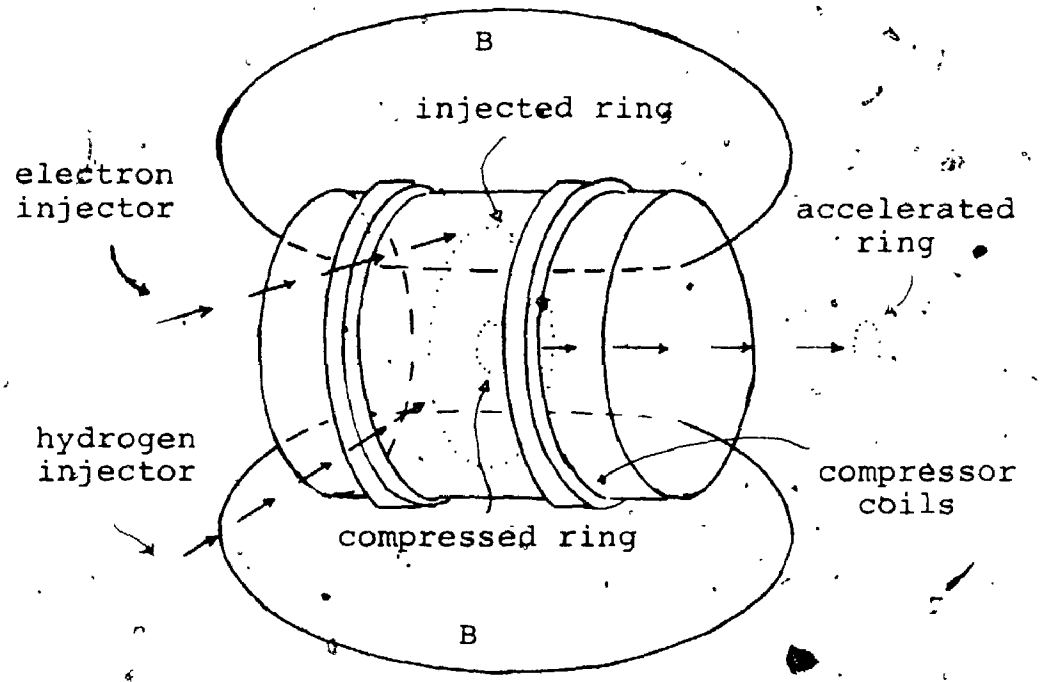

Fig. 1. Pulsed field compressor.

angles to the field(fig. 1). Then hydrogen gas is injected; it becomes ionized by the intense circulating beam of electrons, and the protons formed become trapped by the potential well of the electron space charge. At this point the magnetic field is increased from orders of 10^{-1}kG to 10kG, whereby the ring radius shrinks down to about 5cm. Acceleration of the ring is achieved by rf cavities or by passing the ring through a decreasing magnetic field so that rotational energy is transferred into longitudinal energy.

There had been so much work done on the ERA after the 1967 meeting that it was found necessary to hold another one in the following year at Berkeley to discuss new findings by the various groups. In this meeting com-

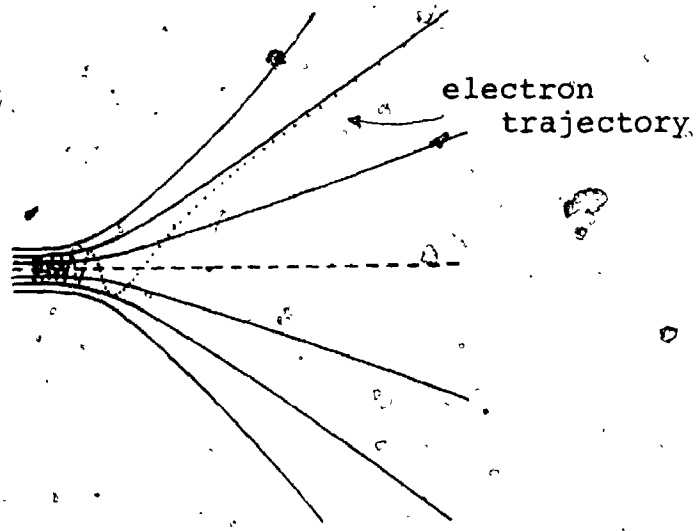

Fig. 2. Solenoidal field compressor.

pression by static field was proposed by Lewis.[16] Similar methods were also put forward by Berg et al.[17] and Laslett et al.[18] The essential feature in these proposals is injection of a straight electron beam into a solenoidal magnetic field(fig. 2). If injection is at an angle to the axis and without a radial component of velocity, the orbit is a conical helix of decreasing pitch, and accumulate into a dense ring configuration with small radius at a suitably high field point along the solenoid.

These static field methods are simpler than the pulsed ones in that no time programming is required. However, they have a common disadvantage of having to use a solenoidal field which has unstable mirror type curvatures.[19] A second disadvantage is in the requirement of injection from a single point into the field with the subsequent formation of a ring at the high field end. This

requirement makes considerable demand on the angle-energy tolerance of the beam. The fact that only one point in azimuth is available for injection means that all the current must come from this point, and this introduces space-charge problems if the beam is to have sufficient current for the formation of a ring.

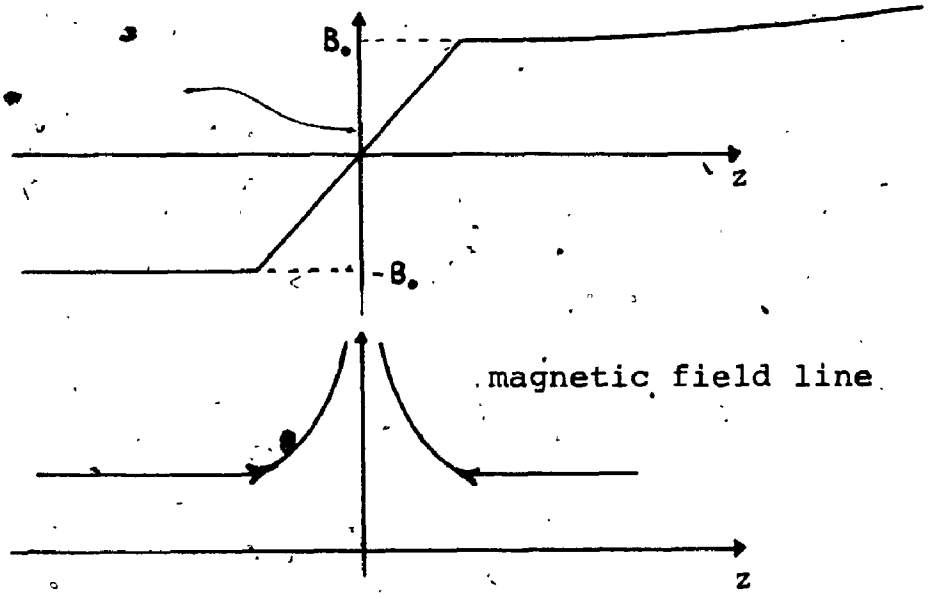

Fig. 3. Cusped field compressor.

An alternative approach to single point injection was first proposed by dePackh.[20] A hollow electron beam is injected from an annular cathode within a region of strong longitudinal magnetic field, and accelerated to an energy of between 10 to 25Mev. The magnetic field is strong enough to make radial and azimuthal motion negligible. The electron beam is then passed through a cusped field in which the direction of the longitudinal magnetic field is reversed in sign, changing from $-B_o$ to $+B_o$ in a

short distance(fig. 3), and thus acquiring some azimuthal velocity at the expense of longitudinal velocity. If the transition of B_z from $-B_o$ to B_o could take place ideally in zero distance, then virtually all of the kinetic energy could be changed from longitudinal to azimuthal while the beam is passing through the cusp. In practice, a short but finite length cusp must exist. Hence only partial conversion is possible, if excessive radial motion is to be avoided in the post-cusp region.

After passing through the cusp, the electron velocity is still predominantly longitudinal, and the electron beam has not yet been 'squashed' into a ring. By letting the magnetic field strength to increase very slowly after the cusp region, further conversion takes place gradually. Since the front portion of the beam undergoes this conversion first, its forward velocity starts to be slowed down first, with the consequence of the beam being squashed into a ring.

Neutral gas atoms are introduced into the path of the electrons in the post-cusp region. They are easily ionized by the rapidly circulating electrons. Since the forward velocity is still appreciable right after passing through the cusp, any ion formed at this stage is left behind. When the longitudinal velocity of the beam is

sufficiently small, it will pick up these ions. The entire system is ready for acceleration when enough ions have been picked up.

An injector has been built at the University of Maryland.[21] It was designed to inject a hollow electron beam of energy 5Mev, with peak current 5kA. The initial tests reported in reference 21 achieved a 2Mev, 6kA beam.

Theoretical investigation of the cusp region had been done by Kalnins et al.,[22] where a single particle approach was used. They found that an iron plate with an annular slit for the passage of the electron beam reduces the length of the cusp, and hence reduces the shift of the centre of the ring off the axis. Radial loss of electrons at the symmetry plane of the cusp poses a serious problem in this region. Striffler et al.[23] studied the effect of applying a negative voltage on a section of the surrounding cylindrical conductor in the region of the cusp. They calculated the limits of the allowable applied voltage. It must not be too low so that effective radial confinement is possible, and must not be too high so that electrons can pass through the cusp. They also gave a plot of the distribution of electrons in the cusp region for various lengths of applied voltage. When this length is equal to the radius of the cylindrical conductor, the

electrons cannot pass through.

Most of the papers[24-26] dealing with the post-cusp regions considered a stationary electron ring confined in a constant magnetic field $\underline{B}=B_o\hat{z}$. The ions were treated as a background which either neutralizes the electron ring,[24] or provides a space charge electric field only.[25,26] Equilibrium properties concerning the major radius R, the ring envelope, and the inclusion of a conducting wall had been obtained. The motion of the ions, and the longitudinal motion of the ring along a space dependent magnetic field on top of the motions in the rest frame of the ring have been considered analytically by Ehrman[27] only recently. According to the validity of the various approximations that can be made, he described the development of the electron beam after passing through the cusp in terms of 5 stages, and considered the third stage in detail.

This is the stage when the forward motion is the slowest, and includes much of the ion pick-up region. The characteristics of this stage are the adiabatic invariance of the longitudinal and radial action integrals, $\oint P_z dz$ and $\oint P_r dr$, for both kinds of particles in the ring frame. The existence of these invariants implies the use of two time scales in the solution of the problem. In the long time scale(LTS), the only invariants are the

action integrals, however, in the short time scale(STS) there exist other physical quantities whose time dependence is slow enough so that they are not changed appreciably over many electron or ion bounce times.

In reference 27, Ehrman first obtained quasi-equilibrium distributions by neglecting the time dependence of the STS Vlasov equations; LTS time dependence was obtained by matching different STS solutions. The present thesis considers the fast time dependence of two of the STS equilibria. A brief discussion of the equilibrium problem is presented in section 2. It must be emphasized that the discussion is confined to those matters that are relevant to the present thesis only; no attempt is made to summarize the entire of reference 27. In section 3 linear perturbation theory is applied to the equilibrium equations given in section 2 with the inclusion of the fast time dependence. It turns out that all information on stability is contained in a Fredholm integral equation. Section 3 deals with the derivation of this equation, while section 4 simplifies the kernel to a more tractable form. With the aid of this Fredholm equation we consider the stability of the system in section 5. Since r dependence has been neglected, the stability analysis applies to the z motion only. While it is foreseeable that there are instabilities due to the radial and azimuthal perturbations, they will not show up in the present analysis.

2. STS Equilibria.

In the third stage the forward velocity $\beta_z = v_z/c$ of the electron beam has been slowed down considerbly, so that β_z^2 may be neglected compared to 1, and γ_z may be replaced by 1. In the rest frame of the ring γ_θ' is related to γ by

$$\gamma_\theta' = \gamma/\gamma_z, \tag{2.1}$$

where the γ's have their usual meaning in the special theory of relativity, the primed variables refer to the ring frame, and the subscripts refer to the cylindrical coordinates (r,θ,z), with z being in the direction of the external magnetic field. Since γ_z may be replaced by 1, γ_θ' and γ can be used interchangeably in this stage.

We assume that the ratio of Budker's parameter ν=(linear electron density along ring circumference)x (e^2/mc^2), to γ is negligible compared to 1, that is

$$\nu/\gamma \ll 1. \tag{2.2}$$

This assumption has its basis in existing experiments.[28] Kegel[29] and Schmidt[30] showed that it implies the self-fields are sufficiently weak that the equilibrium ring radius R is equal, in a first approximation, to the Lamor radius of a single electron with energy γmc^2. Since the ring travels in a very slowly increasing magnetic field in stage three, we may consider R as a STS invariant.

As the beam slows down gradually after passing through the cusp, ions are being picked up. We consider the third stage is reached when there have been enough ions picked up, so that, in the ring frame, the z-action integral and the r-action integral of an electron are good adiabatic invariant, and that the following inequality holds

$$\gamma^{-2} << f << 1, \tag{2.3}$$

where $f=N_i/N_e$; N_i, N_e being the total number of ions and electrons in the ring. This inequality implies that each species in the ring 'sees' the field produced by the other species only. For the ions, since $f<<1$, there are not many of them in the ring, hence the field produced by them are overwhelmed by those of the electrons. On the other hand, the electrons experience a γ^{-2} cancellation of their mutual repulsion[31] due to their relativistic motion, and since $\gamma_\theta'^{-2} \simeq \gamma^{-2} << f$ the residual repulsive field is negligible as compared with the attractive field of the ions. Besides the field due to the ions, the electrons are affected by the external magnetic field also, whereas the ions, having a negligible θ velocity, are insensitive to it.

In the ring frame, each particle thus oscillates within the ring in a field produced by the particles of the other kind only (and, for electrons, in the external field). If the bounce times of the particles trapped in

the wells are short compared with the average times characterizing the wells, we can consider the longitudinal and radial action integrals as good adiabatic invariants. These invariants are essential to the LTS equilibrium analysis. For the present STS stability problem, we take the oscillation periods as a standard of time, since any change in the field quantities must effect a change in these periods.

In order to make the mathematical analysis a little simpler the filament model assumes that

$$r_o << z_o << R, \tag{2.4}$$

where $2r_o$ and $2z_o$ are the ring extensions in r and z. In an actual ERA,[28] $z_o << R$ should be a good assumption in stage three, but $r_o << z_o$ may well be violated, and r_o may be comparable to z_o. The latter assumption was made to simplify the mathematics of the actual system, so that the solutions to this simplified problem can be used as input into a program which drops this assumption.

Equation (2.4) means that the electron-ion ring is considered to consist of almost straight filaments of charge and current having a length $2\pi R$, and all being located at $r=R$, with a distribution in density and z-momentum along z. The condition $z_o << R$ means that curvature effects are being neglected, though the value of R does appear as constant in the equations that we shall be dealing with. We also assume that all STS equilibrium distributions are independent of θ, and that the ions are considered to have no θvelocity, while

the electrons all have a ring frame θ velocity β_θ' which is invariant on STS.

The above assumptions mean that the single particle distribution functions of electrons and ions can be written as

$$\delta(r-R)\delta(P_r)\delta(P_\theta - R\alpha)f_e(z,P_z,t),$$

$$\delta(r-R)\delta(P_r)\delta(P_\theta)f_i(z,P_z,t),$$

where the δ's are Dirac delta functions, the subscripts 'e' and 'i' refer to electron and ion respectively, $R\alpha$ is the constant θ canonical momentum, and $(r,\theta,z,P_r,P_\theta,P_z)$ are space variables and their corresponding canonical momenta in the ring frame. Since we will not be using the laboratory frame any more, the primes in the ring frame variables have been dropped. After integrating over the appropriate phase-space variables, all we have to consider are the functions $f_e(z,P_z,t)$ and $f_i(z,P_z,t)$, and the Vlasov equations for each species are

$$\frac{\partial f}{\partial t}e + \frac{P_z}{m\gamma}\frac{\partial f}{\partial z}e - e(E_z-\beta_\theta B_r)\frac{\partial f}{\partial P_z}e = 0, \qquad (2.5)$$

$$\frac{\partial f}{\partial t}i + \frac{P_z}{M}\frac{\partial f}{\partial z}i + eE_z\frac{\partial f}{\partial P_z}i = 0. \qquad (2.6)$$

The coefficient of $-e\partial f_e/\partial P_z$ may be rewritten thus

$$E_z-\beta_\theta B_r = E_{zi} + (E_{ze}-\beta_\theta B_{re}) - \beta_\theta B_r^{ext},$$

$$\simeq E_{zi} - \beta_\theta B_r^{ext},$$

$$= -\partial\Phi_i/\partial z + \beta_\theta B_r^{ext},$$

where E_{zi}, E_ze are the electric fields due to ions and

electrons respectively, B_{re} is the internal B_r due to electrons, while B_r^{ext} is the external r component of magnetic field. Furthermore β_θ is considered a constant on STS. The neglect of $E_{ze}-\beta_\theta B_{re}$ compared to E_{zi} requires the $\gamma^{-2} << f$ condition of equation (2.3). Similarly, the coefficient of $e\frac{\partial f_i}{\partial P_z}$ may be rewritten

$$E_z = E_{zi} + E_{ze} \simeq E_{ze} = -\frac{\partial \Phi_e}{\partial z},$$

since $f<<1$.

The term $\beta_\theta B_r$ in equation (2.5) accounts for the effect of the external magnetic field on the electrons. In the course of the equilibrium analysis given in reference 27, it became apparent that the inclusion of this term introduces small odd terms in the potential and charge density function. These non-even functions give rise to a problem of single-valuedness to one of the equations: equation 31 of reference 27 (In order to avoid the repetitive phrase 'of reference 27', all equations from that reference will be quoted without brackets and without decimal to distinguish them from the equations of the present thesis). While it is possible to resolve this problem, the self-consistent solution obtained in section 5 of reference 27 is far from being trivial. On the other hand, some of the solutions obtained by leaving out the odd terms are simple delta and step functions. Since the object of the present thesis is to analyse the stability of the latter solutions,

we shall drop the magnetic term, and rewrite equations (2.5) and (2.6) as

$$\frac{\partial f_e}{\partial t} + \frac{P_z}{m\gamma}\cdot\frac{\partial f_e}{\partial z} + e\frac{\partial \Phi_i}{\partial z}\cdot\frac{\partial f_e}{\partial P_z} = 0, \qquad (2.7)$$

$$\frac{\partial f_i}{\partial t} + \frac{P_z}{M}\cdot\frac{\partial f_i}{\partial z} - e\frac{\partial \Phi_e}{\partial z}\cdot\frac{\partial f_i}{\partial P_z} = 0. \qquad (2.8)$$

Since the potential function in the electron Vlasov equation is the potential due to the ions, and the other way round for the ion Vlasov equation, they represent a pair of coupled equations. The coupling is more apparent if we write down the expressions for the potentials and surface charge densities

$$\Phi_e(z,t) = 2\int_{-\infty}^{\infty} dz'\sigma_e(z',t)\log(8R/|z-z'|), \qquad (2.9)$$

$$\Phi_i(z,t) = 2\int_{-\infty}^{\infty} dz'\sigma_i(z',t)\log(8R/|z-z'|), \qquad (2.10)$$

$$\sigma_e(z,t) = -\frac{e}{R}\int_{-\infty}^{\infty} dP_z f_e(z,P_z,t), \qquad (2.11)$$

$$\sigma_i(z,t) = \frac{e}{R}\int_{-\infty}^{\infty} dP_z f_i(z,P_z,t), \qquad (2.12)$$

where the Φ's are obtained from elementary electrostatics, and are valid for $|z-z'| << \pi R$, which is within the limits of the present consideration. It must be noted that the time dependence of these functions were dropped in the equilibrium analysis.

The method employed by reference 27 to solve the equilibrium problem was to assume an electron distribution, an electron charge density, an ion potential outside of the

ring, and an untrapped ion distribution. From these assumed quantities, equations (2.7-12) can be solved with the time dependence dropped. While it is not neeessary to repeat the equilibrium analysis all over again, we will write down the equilibrium functions for ease of reference. All these functions will have a superscript (o), to distinguish them from the perturbed quantities with superscript (1). The functions given below are not identical to those of reference 27 in the sense that there they were made as general as possible, carrying as many terms as possible in the Tchebycheff expansions used; whereas here only zeroth order quantities are included.

The assumed electron distribution is a single dePackh water bag.[9,13,32] Refering to fig. 4, this distribution has a constant positive value, C_o, inside the shaded region, and is zero outside. Mathematically, it can be expressed as

$$f_e^{(o)}(H_e) = C_o[U(C_2-H_e)+U(H_e-C_1)-1],$$

where $U(x)$ is the unit step function, H_e is the electron Hamiltonian, and C_1, C_2 are constants with

$$0 > C_2 > C_1 = \min_{z \text{ in ring}} (-e\Phi_i(z)).$$

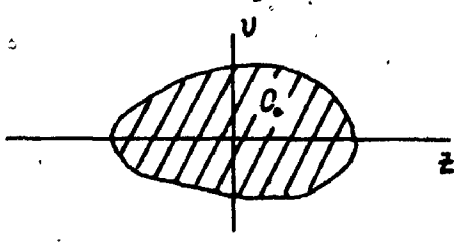

Fig. 4. A water bag distribution.

This is the form used in reference 27. However for the stability analysis, it is more convenient to express it in terms of the equilibrium velocity $\pm w(z)$ of the most energetic electrons,

$$f_e^{(o)}(z,v) = C_o[U(v+w)-U(v-w)] \qquad (2.13)$$

The usefulness of the water bag arises from the fact that we can neglect collisions in the electron Vlasov equation, so that by Liouville's theorem, the phase space enclosed by the water bag is incompressible, and a perturbation can only change its shape, thus simplifying the solution of the time dependent Vlasov equation.

The equilibrium electron surface charge density, the electron potential, and the ion potential are given by equations 22, 61b and 26a. They are rewritten for ease of reference as the following

$$\sigma_e^{(o)}(x) = \begin{cases} -\frac{2e}{R}\sqrt{2m\gamma}C_o z_o b_o \sqrt{1-x^2}\left(1 + \sum_{n=1}^{\infty}\beta_n U_n(x)\right), & |x|<1 \\ 0, & |x|>1 \end{cases}$$

$$e\phi_e^{(o)}(x) = e\phi_e(0) + \frac{e^2 N_e}{\pi R}\left(x^2/2 + \beta_2(x^4-3x^2/2)\right), \quad |x|<1$$

$$e\phi_i^{(o)}(x) = -C_2 + z_o^2 b_o^2(1-x^2)\left(1 + \sum_{n=1}^{\infty}\beta_n U_n(x)\right)^2, \quad |x|<1$$

where $N_e = 2\pi^2\sqrt{2m\gamma}b_o C_o z_o^2$ is the total number of electrons in the ring, and we have normalized the z coordinate by setting $x=z/z_o$, and b_o is a constant defined by equation 22a. It turns out that the potentials outside of the ring do not

come into the stability analysis, hence they are left out from the above equations. Setting $\beta_n=0$, for all $n\geq 1$, we get

$$\sigma_e^{(o)}(x) = \begin{cases} -\frac{eN_e}{\pi^2 R z_o}\sqrt{1-x^2}, & |x|\leq 1, \\ 0 & |x|>1, \end{cases} \qquad (2.14)$$

$$e\phi_e^{(o)}(x) = e\phi_e^{(o)}(o) + \frac{e^2 N_e}{\pi R}\cdot x^2, \quad |x|<1 \qquad (2.15)$$

$$e\phi_i^{(o)}(x) = -C_2 + z_o^2 b_o^2(1-x^2), \quad |x|<1, \qquad (2.16)$$

Depending on whether or not we want to assume there are ions piled up at the ends $\pm z_o$, the ion distribution function given by equation 65a reduces to

$$f_i^{(o)}(H_i) = BU(H_i^{max}-H_i), \qquad (2.17)$$

$$f_i^{(o)}(H_i) = A\delta(H_i^{max}-H_i) + BU(H_i^{max}-H_i), \qquad (2,18)$$

where H_i is the ion Hamiltonian, and

$$A = \frac{1}{2\pi}\sqrt{\frac{b_o C_o R}{\pi M}}\sqrt{2m\gamma}\cdot\frac{\pi b_o^2 z_o^2}{e}\cdot\left(\frac{e^2 N_i}{\pi b_o^2 z_o^2 R} - 1\right), \qquad (2.19)$$

$$B = \frac{1}{2\pi}\sqrt{\frac{b_o C_o R}{\pi M}}\sqrt{2m\gamma}\cdot\frac{\pi b_o^2 z_o^2}{e}\cdot\frac{\pi R}{e^2 N_e}, \qquad (2.20)$$

With N_i being the total number of ions. Equation (2.17) gives the soltion for no pile up at the ends, and for this solution to be valid equation 44 must hold, that is

$$N_i = \frac{\pi b_o^2 z_o^2 R}{e^2}. \qquad (2.21)$$

If this is not true, then the ion distribution function is given by equation (2.18). Since A must be non-negative as required by the definition of a distribution function, we

must have

$$N_i > \frac{\pi b_o^2 z_o^2 R}{e^2}. \qquad (2.22)$$

In general we do not wish to impose equations (2.21).

From equations (2.17,18), the corresponding ion surface charge densities are found to be

$$\sigma_i^{(o)}(x) = \frac{eN_i}{\pi^2 R z_o} \sqrt{1-x^2},$$

and,

$$\sigma_i^{(o)}(x) = \frac{b_o^2 z_o^2}{2\pi eR} \cdot \left[\left(\frac{e^2 N_i}{\pi b_o^2 z_o^2 R} - 1 \right) - 2x^2 \right] \Big/ \sqrt{1-x^2}.$$

The schematic behaviour of these density functions are shown in the following figures.

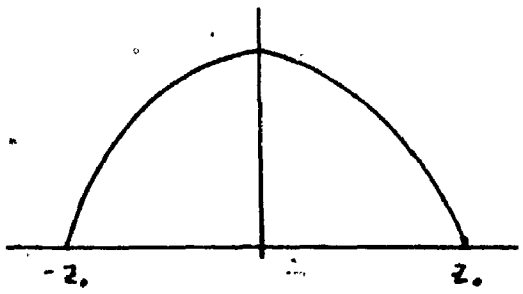

no pile up of ions

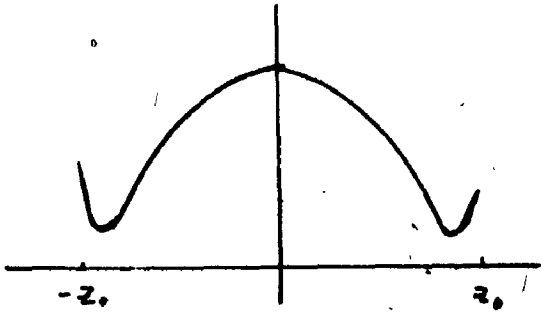

pile up of ions

3. Linearized Perturbation.

The time dependence of the solutions of equations (2.7) and (2.8) can be obtained by doing an exercise in mathematical merry-go-round with the aid of equations (2.9-12). First of all we follow the tradition of water bag users,[9,13] by considering perturbations that distort the contour of the water bag in fig. 4, and write the perturbed distribution function as

$$f_e = C_o[U(v+w-u_-(x,t)) - U(v-w-u_+(x,t))] \qquad (3.1)$$

where $u_\pm$ are the perturbations on the upper ($v_z>0$) and lower ($v_z<0$) contour of fig. 4. By defining a new quantity $T_\pm = \pm\gamma m w u_\pm$ which is proportional to the perturbed kinetic energy of the electrons, we obtain an equation for each of the $T_\pm$. Since they have the same form, we drop the subscripts $\pm$. After taking the Laplace transform, it can be solved formally, in the sense that the rhs contains an unknown $\hat{\Phi}_i^{(1)}$, which can be expressed in terms of another unknown $\hat{f}_i^{(1)}$, which can be expressed in terms of another unknown $\hat{\Phi}_e^{(1)}$, which can be expressed in terms of the original $\hat{T}$ we started with, and by substituting in the reversed order we obtain an inhomogeneous Fredholm equation of the second kind in $\hat{T}$. The head in each of the functions denotes its Laplace transform.

The linearized form of equation (2.7) for first order quantities, obtained by substituting equation (3.1)

for f_e and dropping the second order quantities, is

$$\frac{\partial}{\partial t}\gamma m u_{\pm} \pm \frac{1}{z_o}\frac{\partial}{\partial x}(\gamma m w u_{\pm}) = \frac{e}{z_o}\frac{\partial}{\partial x}\phi_i^{(1)}(x,t), \qquad (3.2)$$

where the variable x is used instead of z, and we have assumed that each of the perturbed quantities $\phi_{i,e}$, $\sigma_{i,e}$ and f_i can be broken into a sum of an equilibrium quantity plus a first order perturbed term

$$g(x,t) = g^{(o)}(x) + g^{(1)}(x,t).$$

By defining

$$T_{\pm}(x,t) = \pm\gamma m w u_{\pm}(x,t), \qquad (3.3)$$

and

$$\phi(x) = \begin{cases} z_o \int_{-1}^{x} \frac{dx'}{w(x')}, & v_z > 0, \\ \phi_o - z_o \int_{-1}^{x} \frac{dx'}{w(x')}, & v_z < 0, \end{cases} \qquad (3.4)$$

$$\phi_o = 2\phi(1),$$

= oscillation period of the most energetic electrons,

equation (3.2) can be transformed into

$$\pm\frac{\partial T_{\pm}}{\partial t} \pm \frac{\partial T_{\pm}}{\partial \phi} = \pm e\frac{\partial \phi_i^{(1)}(\phi,t)}{\partial \phi}.$$

Since each of these equations has the same form, we drop the subscripts ±, and write

$$\frac{\partial T}{\partial t} + \frac{\partial T}{\partial \phi} = e\frac{\partial \phi_i^{(1)}(\phi,t)}{\partial \phi}, \qquad (3.5)$$

with the understanding that

$$T(\phi,t) = \begin{cases} T_+ , & 0 \le \phi < \phi_o/2 \\ T_- , & \phi_o/2 \le \phi < \phi_o \end{cases} \tag{3.6}$$

It can be solved formally by the standard Laplace transform method

$$\hat{T}(\phi,s) = e^{-s\phi}\{ \frac{1}{e^{s\phi_o}-1} \int_0^{\phi_o} d\phi' e^{s\phi'} T(\phi',0) + \int_0^{\phi} d\phi' e^{s\phi'} T(\phi',0) + \frac{1}{e^{s\phi_o}-1} \int_0^{\phi_o} d\phi' e^{s\phi'} e \frac{\partial \hat{\Phi}_i^{(1)}}{\partial \phi'} + \int_0^{\phi} d\phi' e^{s\phi'} e \frac{\partial \hat{\Phi}_i^{(1)}}{\partial \phi'} \}, \tag{3.7}$$

where the head denotes a Laplace transformed function

$$\hat{g}(y,s) = \int_0^{\infty} dt\, e^{-st}\, g(y,t), \tag{3.8}$$

$T(\phi,0)$ is the initial perturbation, and the continuity of T at the ends, that is $T(0,s)=T(\phi_o,s)$, is assumed. The letter 'e' was used to mean both the basic unit of electronic charge and the exponential symbol; their meaning can be understood from context.

The unknown $\hat{\Phi}_i^{(1)}$ on the rhs can be found in terms of $\hat{f}_i^{(1)}$ with the aid of equations (2.10) and (2.12). We first change the integration variable of (2.12) into H_i instead of P_z by the relation $dP_z = \pm dH_i / \sqrt{2/M(H_i - e\Phi_e^{(o)}(\vec{x}))}$

$$\hat{\sigma}_i^{(1)}(\vec{x},s) = \frac{e}{R_{e\Phi_e^{(o)}(\vec{x})}} \int_{}^{\infty} dH_i \frac{(f_{i+}^{(1)} + f_{i-}^{(1)})}{\sqrt{2/M(H_i - e\Phi_e^{(o)}(\vec{x}))}},$$

where $\hat{f}_{i\pm}^{(1)}$ are perturbed distribution functions for $v_z \gtrless 0$. Substituting this into equation (2.10), we get

$$\hat{\Phi}_i^{(1)}(x',s) = \frac{2ez_o}{R}\int_{-1}^{1} dx'' \log\frac{8R/z_o}{|x'-x''|}\int_{e\Phi_e^{(o)}(x'')}^{\infty} dH_i \frac{(\hat{f}_{i+}^{(1)} + \hat{f}_{i-}^{(1)})}{\sqrt{2/M(H_i - e\Phi_e^{(o)}(x''))}}. \tag{3.9}$$

We have assumed that the ions do not go over the ends $\pm z_o$ even in the perturbed state, hence, the x integral takes the limits ± 1. If we define a new quantity τ, similar to ϕ of the electrons by

$$\tau = \begin{cases} z_o \int_{-x_o}^{x} \frac{dx'}{\sqrt{2/M(H_i - e\Phi_e^{(o)}(x'))}}, & v_z > 0, \\ \tau_o - z_o \int_{-x_o}^{x} \frac{dx'}{\sqrt{2/M(H_i - e\Phi_e^{(o)}(x'))}}, & v_z < 0, \end{cases} \tag{3.10}$$

$\tau_o = 2\tau(x_o, H_i)$,

= period of the ions of normalized extension $[-x_o, x_o]$,

and take

$$\hat{f}_i^{(1)} = \begin{cases} \hat{f}_{i+}^{(1)}, & 0 < \tau < \tau_o/2, \\ \hat{f}_{i-}^{(1)}, & \tau_o/2 < \tau < \tau_o, \end{cases} \tag{3.11}$$

then equation (3.9) can be written as

$$\hat{\Phi}_i^{(1)}(x,s) = (2e/R)\int_0^{\tau_o} d\tau \sqrt{(H_i^{max} - e\Phi_e^{(o)}(\tau))} \log\frac{8R/z_o}{|x'-x''|} \cdot \int_{e\Phi_e^{(o)}(x)}^{\infty} \frac{dH_i}{\sqrt{(H_i - e\Phi_e^{(o)}(x))}} \hat{f}_i^{(1)},$$

where $\tau = \tau(1, H_i^{max})$. Since this is the only occasion where

we have used τ corresponding to the maximum energy, all future reference to it shall be taken as $\tau = \tau(x_o, H_i)$. Taking derivative with respect to ϕ', and changing the order of integration we get

$$\frac{\partial \hat{\phi}_i^{(1)}(\phi', s)}{\partial \phi'} = -\frac{2e}{Rz_o} \operatorname{sgn}(\phi') w(\phi') \int_{H_i^{min}}^{\infty} dH_i \int_0^{\tau_o} d\tau \frac{\hat{f}_i^{(1)}(\tau, H_i, s)}{\dot{x}(\phi') - \dot{x}(\tau)}, \tag{3.12}$$

where

$$\operatorname{sgn}(\phi) = \begin{cases} +1, & 0 \leq \phi < \phi_o/2, \\ -1, & \phi_o/2 \leq \phi < \phi_o \end{cases}, \tag{3.13}$$

and the bar in the τ integral means Cauchy's Principal value.

While it is possible to solve the linearized form of equation (2.8) formally as we did with that of equation (2.7), the solution will lead to a very unpleasant integration in the Fredholm kernel which will be developed. To avoid this integration, we do not use the Laplace transform method here, but rather, we do a Fourier expansion of $\hat{f}_i^{(1)}$, and solve it in terms of its Fourier components. This procedure immediately raises two questions. The first being why not the other way round, that is, to expand $\hat{T}$ and solve for $\hat{f}_i^{(1)}$? And, second, why not treat them equally, that is expand both in terms of Fourier series? The answer to the former is easy, because by doing so we cannot avoid the anticipated difficult integration in τ. The answer to the latter is less obvious, but we will show in

Appendix A that it is equivalent to the present method. As will be seen in the appendix that there is no obvious advantage of one method over the other, the method we presented here just happens to be the first one we attempted.

Let us return from our digression, and transform the variables (x,P_z,t) of equation (2.8) into (τ,H_i,t) with the aid of equation (3.11) and the relation $H_i=P_z^2/2M + e\Phi_e^{(o)}(x)$. In terms of (τ,H_i,t), equation (2.8) become

$$\frac{\partial f_i}{\partial t} + \left(e\frac{\partial}{\partial \tau}\Phi_e^{(o)}(\tau)\frac{\partial}{\partial H_i} + \frac{\partial}{\partial \tau}\right) f_i - e\frac{\partial}{\partial \tau}\Phi_e(\tau)\frac{\partial}{\partial H_i} f_i = 0,$$

that is,

$$\frac{\partial f_i}{\partial t} + \frac{\partial f_i}{\partial \tau} + e\frac{\partial}{\partial \tau}\left(\Phi_e^{(o)}(\tau) - \Phi_e(\tau,t)\right)\frac{\partial}{\partial H_i} f_i = 0,$$

where f_i takes the same meaning as $\hat{f}_i^{(1)}$ in equation (3.12). Dropping the second order terms from the above equation, we get

$$\frac{\partial f_i^{(1)}}{\partial t} + \frac{\partial f_i^{(1)}}{\partial \tau} = e\frac{\partial}{\partial \tau}\Phi_e^{(1)}(\tau,t)\frac{d}{dH_i} f_i^{(o)}(H_i), \tag{3.14}$$

and its Laplace transform is

$$s\hat{f}_i^{(1)} + \frac{\partial \hat{f}_i^{(1)}}{\partial \tau} = f_i^{(1)}(\tau,H_i,0) + e\frac{\partial \hat{\Phi}_e^{(1)}(\tau,t)}{\partial \tau}\frac{d}{dH_i} f_i^{(o)}(H_i) \tag{3.15}$$

where $f_i^{(1)}(\tau,H_i,0)$ is the initial perturbation. Here we depart from the method followed in solving for $\hat{T}$, and

expand $\hat{f}_i^{(1)}$

$$\hat{f}_i^{(1)}(\tau,H_i,s) = \sum_{n=-\infty}^{\infty} e^{in\tau/\bar{\tau}_0}\hat{f}_n(H_i,s), \qquad (3.16)$$

where $\bar{\tau}_0=\tau_0/2\pi$. It will be shown in the following section that τ_0 is independent of H_i (this is true for the present class of solutions only; in general, it is not necessary so.), and hence $\hat{f}_n(H_i,s)$ contain all the H_i dependence of $\hat{f}_i^{(1)}$. $\hat{f}_i^{(1)}$ can be easily obtained from equation (3.15) by the orthogonality property of the Fourier expansion

$$\hat{f}_i^{(1)}(\tau,H_i,s) = \sum_{n=-\infty}^{\infty} \frac{e^{in\tau/\bar{\tau}_0}}{\tau_0(in/\bar{\tau}_0+s)} \int_0^{\tau_0} d\tau' e^{-in\tau'/\bar{\tau}_0}\left(f_i^{(1)}(\tau',H_i,0) + e\frac{\partial\hat{\phi}_e^{(1)}}{\partial\tau'}\frac{df_i^{(o)}}{dH_i}\right). \qquad (3.17)$$

The last of the unknowns in our merry-go-round can be obtained by differentiating the first order quantity of equation (2.9)

$$\phi_e^{(1)}(x,t) = 2z_o \int_{-\infty}^{\infty} dx' \, \sigma_e^{(1)}(x',t)\log\frac{8R/z_o}{|x-x'|}, \qquad (3.18)$$

and the charge density is given by equation (2.11), after substituting $f_e(x,P_z,t)$ from equation (3.1)

$$\sigma_e(x',t) = -\frac{2em\gamma C_o}{R}w(x') - \frac{em\gamma C_o}{R}(u_+-u_-). \qquad (3.19)$$

The first term is recognized as the equilibrium charge density, and the second is the first order perturbed density

which can be expressed in terms of T± defined in equation (3.3)

$$\sigma_e^{(1)}(x,t) = -\frac{eC_o}{Rw}(T_+ + T_-).$$

Substituting this into (3.18) and differentiating with respect to τ we get

$$\frac{\partial \Phi_e^{(1)}}{\partial \tau} = \frac{2eC_o}{Rz_o}\,\mathrm{sgn}(\tau)\sqrt{2/M(H_i - e\Phi_e^{(o)}(\tau))}\int_0^{\phi_o} d\phi\,\frac{\hat{T}(\phi,s)}{x(\tau)-x(\phi)}, \quad (3.20)$$

where sgn(τ) denotes the similar sign changes as its counter part sgn(φ),

$$\mathrm{sgn}(\tau) = \begin{cases} +1, & 0<\tau<\tau_o/2, \\ -1, & \tau_o/2<\tau<\tau_o \end{cases},$$

and we have used the Laplace transformed functions. The x integration in (3.18) has been changed into φ, resulting in $\hat{T}(\phi,s)$ of equation (3.7) instead of $\hat{T}_\pm$ in the numerator.

Finally we substitute equation (3.20) into (3.17), then the resulting expression into (3.12), and next the expression resulting from the previous operation into (3.7), and hence obtain the following inhomogeneous Fredholm equation of the second kind

$$\hat{T}(\phi,s) = I[T;f_i] + \int_0^{\phi_o} d\phi''\, K(\phi,\phi'',s)\hat{T}(\phi'',s), \quad (3.21)$$

where the inhomogeneous term is given by

$$I[T;f_i^{(1)}] = e^{-s\phi}\left[\frac{I_T(\phi_o,s)}{e^{s\phi_o}-1} + I_T(\phi,s) + \frac{I_f(\phi_o,s)}{s^{s\phi_o}-1} + I_f(\phi,s)\right], \tag{3.22}$$

with

$$I_T(\phi,s) = \int_0^{\phi_o} d\phi'\, e^{s\phi'} T(\phi',0), \tag{3.23}$$

$$I_f(\phi,s) = -\frac{2e^2}{Rz_o}\int_0^{\phi} d\phi'\, e^{s\phi'}\mathrm{sgn}(\phi')w(\phi')\int_{H_i^{min}}^{\infty} dH_i \int_0^{\tau_o}\frac{d\tau}{\dot{x}(\phi')-x(\tau)}$$
$$\sum_{n=-\infty}^{\infty}\frac{e^{in\tau/\bar{\tau}_o}}{\tau_o(in/\bar{\tau}_o+s)}\int_0^{\tau_o} d\tau'\, e^{-in\tau'/\bar{\tau}_o} f_i^{(1)}(\tau',H_i,0); \tag{3.24}$$

and the kernel is

$$K(\phi,\phi'',s) = e^{-s\phi}\left[\frac{J(\phi_o,\phi'',s)}{e^{s\phi_o}-1} + J(\phi,\phi'',s)\right], \tag{3.25}$$

with

$$J(\phi,\phi'',s) = -\frac{4e^4 C_o}{R^2 z_o^2}\int_0^{\phi} d\phi'\, e^{s\phi'}\mathrm{sgn}(\phi')w(\phi')\int_{H_i^{min}}^{\infty} dH_i \frac{df_i^{(o)}}{dH_i}$$
$$\sum_{n=-\infty}^{\infty} g_n(\phi')h_n(\phi''), \tag{3.26}$$

$$g_n(\phi') = \int_0^{\tau_o} d\tau \frac{e^{in\tau/\bar{\tau}_o}}{\dot{x}(\phi')-x(\tau)}, \tag{3.27}$$

$$h_n(\phi'') = \frac{1}{\tau_o(in/\bar{\tau}_o+s)}\int_0^{\tau_o} d\tau'' \frac{e^{-in\tau''/\bar{\tau}_o}\mathrm{sgn}(\dot{\tau}'')\sqrt{2/M(H_i-e\Phi_e^{(o)}(\tau''))}}{\dot{x}(\tau'') - \dot{x}(\phi'')}. \tag{3.28}$$

4. The Fredholm Kernel.

All the integrals in equation (3.26-28) are rather straightforward to evaluate, although some of the intermediate steps are quite tedious. We will start from the integration of equations (3.27,28) first. Their integrated forms allow the double infinite sum in (3.26) to be reduced to a single infinite sum. It is the derivative of the delta function in $df_i^{(o)}(H_i)/dH_i$ that causes most of the trouble in equation (3.26). After sorting out the various terms in the H_i integration the remaining steps involve only manipulation of trigonometric functions. It turns out that in simplifying the derivative with respect to H_i, the odd and even terms reduce to different but similar forms. The derivation of the n=odd=(2p+1)th term will be presented, and the result of the n=even term will be quoted at the end of this section.

As the integrals of (3.27,28) are in terms of τ, we have to find $x(\tau)$ and $\mathrm{sgn}(\tau)\sqrt{2/M(H_i-e\Phi_e^{(o)}(\tau))}$ in terms of τ first. Since $H_i=e\Phi_e^{(o)}(x_o)$ for ions of normalized extension $[-x_o,x_o]$, we obtain $(H_i-e\Phi_e^{(o)}(x))$ in terms of x by equation (2.15)

$$H_i-e\Phi_e^{(o)}(x) = \frac{e^2N_e}{\pi R}(x_o^2-x^2). \qquad (4.1)$$

Substituting this into equation (3.10) we get

$$x(\tau) = -x_o \cos \tau/\tilde{\tau}_o, \qquad 0 \leq \tau \leq \tau_o \tag{4.2}$$

$$\tilde{\tau}_o = z_o \sqrt{\frac{\pi RM}{2e^2 N_e}}, \tag{4.3}$$

The rhs of (4.3) shows that τ_o is independent of H_i. This is true the present class of solutions only; in general, we expect τ_o to depend on H_i. It must be observed that (4.2) applies to all τ in the interval $[0, \tau_o]$, because the cosine takes care of the sign changes. Substituting (4.2) into (4.1) we get

$$\text{sgn}(\tau)\sqrt{2/M(H_i - e\phi_e^{(o)}(x))} = x_o(z_o/\tilde{\tau}_o)\sin(\tau/\tilde{\tau}_o), \tag{4.4}$$

Here again, the sign change is being taken care of by the sine.

Taking the expression for $x(\tau)$ and $\text{sgn}(\tau)\sqrt{2/M(H_i - e\phi_e^{(o)}}$ from equations (4.2) and (4.4), and substituting into (3.28) we get

$$h_n(\phi''') = -\frac{z_o}{2\pi\tilde{\tau}_o^2(in/\tilde{\tau}_o + s)} \int_0^{\tau_o} d\tau'' \frac{e^{-in\tau''/\tilde{\tau}_o}\sin\tau''/\tilde{\tau}_o}{\cos\tau''/\tilde{\tau}_o + x''(\phi''')/x_o}.$$

The integrand here is made up of the sum of an even and an odd part about $\tau_o/2$ of which the odd part gives zero contribution; hence for $n>0$,

$$h_n(\phi) = \frac{iz_o}{\tau_o(in/\tilde{\tau}_o + s)} \int_0^{2\pi} d\tau \frac{\sin n\tau . \sin\tau}{\cos\tau + x''(\phi)/x_o},$$

where the interval has been normalized to $[0, 2\pi]$. The integrand can be converted into a standard airfoil equation[33]

by the substitution of $y=\cos\tau$

$$h_n(\phi''') = \frac{i2z_o}{\tau_o(in/\bar{\tau}_o+s)}\int_{-1}^{1} dy\, \frac{\sqrt{1-y^2}\,U_{n-1}(y)}{y+\ddot{x}'''/x_o},$$

$$= -\frac{iz_o}{(in+\bar{\tau}_o s)}\, T_n\left(-\frac{\ddot{x}'''(\phi''')}{x_o}\right), \qquad (4.5)$$

where T and U are the Tchebycheff polynomials of the first and second kind. For $-n<0$, $h_{-n}(\phi)$ can be obtained similarly

$$h_{-n}(\phi''') = \frac{iz_o}{(-in+\bar{\tau}_o s)}\, T_n\left(-\frac{\ddot{x}'''(\phi''')}{x_o}\right). \qquad (4.6)$$

In the integration in $g_n(\phi)$, the odd part vanishes again, and the even part can be converted into the other airfoil equation[33] by the cosine substitution.

$$\int_0^{\tau_o} d\tau \frac{e^{in\tau/\bar{\tau}_o}}{\dot{x}+x_o\cos\tau/\bar{\tau}_o} = (1/x_o)\int_0^{\tau_o} d\tau \frac{\cos n\tau/\bar{\tau}_o}{\dot{x}/x+\cos\tau/\bar{\tau}_o},$$

$$= \frac{2\bar{\tau}_o}{x_o}\int_{-1}^{1} dy\, \frac{T_n(y)}{\sqrt{1-y^2}(\dot{x}/x_o+y)},$$

$$= \frac{\tau_o}{x_o} U_{n-1}\left(-\frac{\dot{x}(\phi')}{x_o}\right), \qquad (4.7)$$

with $n>0$ and $y=\cos\tau/\bar{\tau}_o$. Since the even part comes from the cosine of the exponential function, for $-n<0$,

$$g_{-n}(\phi') = g_n(\phi').$$

Equations (4.5-7) are valid for $n \neq 0$. When $n=0$, both g_0 and h_0 are zero. In the airfoil equations, the arguments of the Tchebycheff polynomials must be less than 1. That is these equations are valid if $|x'/x_0|$ and $|x''/x_0| < 1$. This condition is clearly not always satisfied, as x' and x'' are the normalized electron position coordinates, and can be larger in magnitude than x_0. To take account of all x' and x'' values we must replace the airfoil equations by the set

$$\int_{-1}^{1} \frac{dz}{z-y} \frac{T_n(z)}{\sqrt{1-z^2}} = \pi\left(U_{n-1}(y) - \frac{\sigma(y) T_n(y)}{\sqrt{y^2-1}}\right), \qquad (4.8a)$$

$$\int_{-1}^{1} \frac{dz}{z-y} \sqrt{1-z^2} U_n(z) = -\pi\left(T_{n+1}(y) - \sigma(y)\sqrt{y^2-1} U_n(y)\right), \qquad (4.8b)$$

with

$$\sigma(y) = \begin{cases} -1, & y < -1, \\ 0, & |y| < 1, \\ +1, & y > +1. \end{cases}$$

The second term on the rhs of equation (4.8a) is discontinuous at $y = \pm 1$. If we use these equations instead of (4.5) and (4.7), then after doing the H_i integration we find the second term in (4.8b) gives zero contribution, but the second term in (4.8a) blows up at the ends $x = \pm 1$. A remedy to this problem is to assume the ions to 'slop over' by a first order small amount ξ at both ends. In the equilibrium solution this merely pushes the δ function in $f_i^{(o)}(H_i)$ to the ends $-1-\xi$, $1+\xi$. In the present problem,

it has the effect of bringing x_o to $1+\xi$ instead of 1 after integrating over H_i. Since $|x'|<1+\xi$, it anulls all the troubles caused by the singular point y=1 in the second term of equation (4.8a), and reduces its contribution to zero. Since ξ is of the first order, its effect will not be felt in the subsequent analysis. In what follows we shall take (4.5) and (4.7) as they are, with the understanding that the above procedure must be taken for a rigorous treatment.

The symmetry of g_n and h_n allows us to collapse the double infinite sum in equation (3.26) by the following

$$\sum_{n=-\infty}^{\infty} g_n(\phi')h_n(\phi'') = \sum_{n=1}^{\infty}(g_n h_n + g_{-n}h_{-n}),$$

$$= \sum_{n=1}^{\infty} -\frac{2z_o n}{n^2+\bar{\tau}_o^2 s^2}\,\xi_n(\phi',\phi''), \qquad (4.9)$$

where

$$\xi_n(\phi',\phi'') = (\tau_o/x_o)U_{n-1}(-x'(\phi')/x_o)T_n(-x''(\phi'')/x_o). \qquad (4.10)$$

Therefore,

$$J(\phi,\phi'',s) = \frac{4e^{-k}C_o}{R^2 z_{oo}^2}\int^{\phi} d\phi'\, e^{s\phi'}\mathrm{sgn}(\phi')w(\phi')\int_{H_i^{min}}^{\infty} dH_i \frac{df_i^{(o)}(H_i)}{dH_i}$$

$$\sum_{n=1}^{\infty}\frac{2z_o n}{n^2+\bar{\tau}_o^2 s^2}\,\xi_n(\phi',\phi'').$$

Changing the order of integration and summation

$$J(\phi',\phi'',s) = \frac{4e^4C_o}{R^2z_o^2}\sum_{n=1}^{\infty}\frac{2z_on}{n^2+\bar{\tau}_o^2s^2}\int_o^{\phi}d\phi'\, e^{s\phi'}sgn(\phi')w(\phi')$$

$$\cdot\int_{H_i^{min}}^{\infty}dH_i\frac{df_i^{(o)}(H_i)}{dH_i}\xi(\phi',\phi'). \qquad (4.11)$$

For the H_i integration we need the derivative of equation (2.18)

$$\frac{df_i^{(o)}(H_i)}{dH_i} = A\delta'(H_i^{max}-H_i) - B\delta(H_i^{max}-H_i),$$

with the prime in the delta function meaning d/dH_i. Substituting this into the H_i integral of the n^{th} term in (4.11)

$$\int_{H_i^{min}}^{\infty}dH_i\,(A\delta'(H_i^{max}-H_i)-B\delta(H_i^{max}-H_i)\xi_n$$

$$= -(Ad/dH_i + B)\xi_n(\phi',\phi'')\Big|_{H_i=H_i^{max}} \qquad (4.12)$$

From equation (4.10), the derivative with respect to H_i is

$$\frac{d}{dH_i}\xi_n = [\frac{d}{dH_i}(\frac{\tau_o}{x_o}U_{n-1}(\frac{x'}{x_o}))]T_n(\frac{x''}{x_o})+\frac{\tau_o}{x_o}U_{n-1}(\frac{x'}{x_o})\frac{d}{dH_i}T_n(\frac{x''}{x_o}). \qquad (4.13)$$

Since x_o is the only H_i dependent factor in $\xi_n(\phi',\phi'')$, the derivatives can be taken with the aid of equation (4.1). For the first term of the above equation, we have

$$\frac{d}{dH_i}(\frac{\tau_o}{x_o}U_n(\frac{x'}{x_o})) = -\frac{\pi R\tau_o}{2x_o^3e^2N_e}(U_{n-1}(\frac{x'}{x_o}) - \frac{x'}{x_o}U'_{n-1}(\frac{x'}{x_o})),$$

where the prime in the Tchebycheff polynomial means derivative with respect to its argument. From the identities of Tchebycheff polynomial given in reference 33, we can transform the second factor into a linear sum of the U's. Since this involves nothing but tedious algebraic manipulations, we leave the detailed derivation in Appendix B. For n=odd=2p+1, p≥0, the above derivative can be reduced to

$$\frac{d}{dH_i}\left(\frac{\tau_o}{x_o}U_{2p}\left(\frac{\dot{x}}{x_o}\right)\right) = -\frac{\pi R\tau_o}{2x_o^3 e^2 N_e}\left[(2p+1)U_{2p}\left(\frac{\dot{x}}{x_o}\right) + 2\sum_{i=0}^{p-1}(2i+1)U_{2i}\left(\frac{\dot{x}}{x_o}\right)\right], \qquad (4.14)$$

where equation (B6) of Appendix B has been used, and for p=0, the summation convention of equation (B2) must be taken.

For the derivative in the second term of equation (4.13) we have

$$\frac{d}{dH_i}T_n\left(\frac{\dddot{x}}{x_o}\right) = \frac{\pi R}{2x_o^2 e^2 N_e}\left(\frac{\dddot{x}}{x_o}\right)T_n'\left(\frac{\dddot{x}}{x_o}\right).$$

Again, we leave the evaluation of $xT_n'(x)$ in Appendix B, and obtain the derivative for the n=(2p+1)th term from equation (B9) as

$$\frac{d}{dH_i}T_{2p+1}\left(\frac{\dddot{x}}{x_o}\right) = -\frac{\pi R}{2x_o^2 e^2 N_e}\left[(2p+1)\sum_{i=1}^{p-1}T_{2i+1}\left(\frac{\dddot{x}}{x_o}\right)\right.$$

$$+ (2p+1)T_{2p+1}(\frac{\bar{x}}{x_o})]. \qquad (4.15)$$

Collecting terms from (4.15), (4.14), (4.13) and substituting into (4.12) we get for n=odd=2p+1, p≥0,

$$\int_{H_i^{min}}^{\infty} dH_i (A\delta'(H_i^{max}-H_i) - B\delta(H_i^{max}-H_i))\xi_{2p+1}$$

$$= \tau_o((2p+1)\tilde{A}-B)U_{2p}(-\acute{x})T_{2p+1}(-\acute{\bar{x}})$$

$$+ \tau_o\tilde{A}[(\sum_{i=0}^{p-1}(2i+1)U_{2i}(-\acute{x}))T_{2p+1}(-\acute{\bar{x}})$$

$$+ (2p+1)U_{2p}(-\acute{x})\sum_{i=1}^{p-1}T_{2i+1}(-\acute{\bar{x}})], \qquad (4.16)$$

where

$$\tilde{A} = (\pi R/e^2 N_e)A, \qquad (4.17)$$

and at $H_i=H_i^{max}$, $x_o=1$. Since the arguments of the Tchebycheff polynomials are $-x(\phi)$ and $-x(\bar{\phi})$, we must find x in terms of ϕ. From equation (3.19) we see that w(x), the equilibrium electron velocity, is proportional to the equilibrium charge density, and from equation (2.14) we get

$$w(x) = (N_e/\pi^2 2m\gamma C_o z_o)\sqrt{1-x^2}.$$

Substituting this into (3.4) and integrating, we obtain

$$x(\phi) = -\cos\phi/\bar{\phi}_o, \qquad 0\leq\phi<\phi_o, \qquad (4.18)$$

$$\bar{\phi}_o = \pi^2 2m\gamma C_o z_o^2/N_e, \qquad (4.19)$$

$$\mathrm{sgn}(\phi)w(\phi) = (z_o/\bar{\phi}_o)\sin\phi/\bar{\phi}_o, \qquad 0\leq\phi<\phi_o. \qquad (4.20)$$

Substituting equation (4.18) into the arguments of the Tchebycheff polynomials in equation (4.16) reduces it to a sum and product of trigonometric functions only

$$\int_{H_i^{min}}^{\infty} dH_i \,(A\delta'(H_i^{max}-H_i)-B\delta(H_i^{max}-H_i))\,\xi_{2p+1}$$

$$= \tau_o\{((2p+1)\tilde{A}-B)\frac{\sin(2p+1)\phi/\bar{\phi}_o}{\sin\phi/\bar{\phi}_o}\cos(2p+1)\phi'''/\bar{\phi}_o$$

$$+\tilde{A}[(\sum_{i=0}^{p-1}(2i+1)\frac{\sin(2i+1)\phi/\bar{\phi}_o}{\sin\phi/\bar{\phi}_o})\cos(2p+1)\phi'''/\bar{\phi}_o$$

$$+(2p+1)\frac{\sin(2p+1)\phi/\bar{\phi}_o}{\sin\phi/\bar{\phi}_o}(\sum_{i=1}^{p-1}\cos(2i+1)\phi'''/\bar{\phi}_o)]\}. \qquad (4.21)$$

Each term on the rhs contains a factor $1/\sin\phi/\bar{\phi}_o$ which cancels the term $\mathrm{sgn}(\phi)w(\phi)=(z_o/\bar{\phi}_o)\sin\phi/\bar{\phi}_o$ in the numerator when we substitute the above equation into equation (4.11). This cancellation reduces the evaluation of ϕ integral to the simple form of

$$\int d\phi\; e^{s\phi}\sin k\phi/\bar{\phi}_o = \bar{\phi}_o^2 e^{s\phi}\frac{(s\sin k\phi/\bar{\phi}_o-(k/\bar{\phi}_o)\cos k\phi/\bar{\phi}_o)}{(k^2+\bar{\phi}_o^2 s^2)}.$$

Substituting (4.20) and (4.21) into (4.11) and integrating according to the above equation we get

$$J(\phi,\phi''',s) = \frac{8e^4C_o\;\tau_o\bar{\phi}_o}{R^2}\sum_{n=1}^{\infty}\frac{n}{(n^2+\bar{\tau}_o^2 s^2)}(\eta_n(\phi,\phi''',s)-\eta_n(0,\phi''',s)) \qquad (4.22)$$

where for n=odd=2p+1, $p\geq 0$,

$$\eta_{2p+1}(\phi,\tilde{\phi},s) = e^{s\phi}\{((2p+1)\tilde{A}-B)sc((2p+1),\phi)\cos(2p+1)\tilde{\phi}/\bar{\phi}_0$$
$$+\tilde{A}[(\sum_{i=0}^{p-1}(2i+1)sc((2i+1),\phi))\cos(2p+1)\tilde{\phi}/\bar{\phi}_0$$
$$+(2p+1)sc((2p+1),\phi)(\sum_{i=0}^{p-1}\cos(2i+1)\tilde{\phi}/\bar{\phi}_0)]\}, \tag{4.23}$$

with

$$sc(k,\phi) = \frac{ssink\phi/\bar{\phi}_0-(k/\bar{\phi}_0)cosk\phi/\bar{\phi}_0}{(k^2+\bar{\phi}_0^2s^2)}, \tag{4.24}$$

and a similar expression for the even n's.

Due to the sum,

$$(\frac{J(\phi_0,\tilde{\phi},s)}{e^{s\phi_0}-1} + J(\phi,\tilde{\phi},s)),$$

in equation (3.25), a great deal of simplification can be achieved in the final form of the kernel. We illustrate this by considering a representative term in each of the $\eta_n(\phi,\tilde{\phi},s)-\eta_n(0,\tilde{\phi},s)$ in equation (4.22). Since $\tilde{\phi}$ stays unchanged in the two terms of the above sum, we want to consider sums of the form

$$[\frac{e^{s\phi_0}sc(k,\phi_0)-sc(k,0)}{e^{s\phi_0}-1} + (e^{s\phi}sc(k,\phi)-sc(k,0))].$$

From the definition of $sc(k,\phi)$ in equation (4.24) we see that $sc(k,\phi_0)=sc(k,0)$; and the above sum is contracted into

$$e^{s\phi}sc(k,\phi).$$

With this simplification in mind, the completely integrated form of the Fredholm kernel is then

$$K(\phi,\dddot{\phi},s) = \sum_{n=1}^{\infty} \frac{n}{\pi(n^2+\bar{\tau}_o^2 s^2)}\,\zeta_n(\phi,\dddot{\phi},s), \tag{4.25}$$

where for n=odd=2p+1, $p \geq 0$,

$$\begin{aligned}\zeta_{2p+1}(\phi,\dddot{\phi},s) = {} & ((2p+1)\varepsilon-1)sc((2p+1),\phi)\cos(2p+1)\dddot{\phi}/\bar{\phi}_o \\ & + \varepsilon[\Big(\sum_{i=0}^{p-1}(2i+1)sc((2i+1),\phi)\Big)\cos(2p+1)\dddot{\phi}/\bar{\phi}_o \\ & + (2p+1)sc((2p+1),\phi)\Big(\sum_{i=0}^{p-1}\cos(2i+1)\dddot{\phi}/\bar{\phi}_o\Big)].\end{aligned} \tag{4.26}$$

In this final expression we have collected the constants from (4.22), (4.23), (4.17), (2.19) and (2.20), with one of them being

$$\begin{aligned}\frac{8e^4C_o\tau_o\bar{\phi}_o}{R^2}\tilde{A} &= \frac{8e^4C_o\tau_o\bar{\phi}_o}{R^2}\cdot\frac{\pi R}{e^2N_e}\cdot A \,, \\ &= \frac{8e^4C_o\tau_o\bar{\phi}_o}{R^2}\cdot\frac{\pi R}{e^2N_e}\cdot\frac{1}{2\pi}\sqrt{\frac{b_oC_oR\sqrt{2m\gamma}}{\pi M}}\cdot\frac{\pi b_o^2z_o^2}{e}\cdot\Big(\frac{e^2N_i}{\pi b_o^2z_o^2R}-1\Big) \,, \\ &= \Big(\frac{e^2N_i}{\pi b_o^2z_o^2R}-1\Big)/\pi \,,\end{aligned}$$

and the other

$$\begin{aligned}\frac{8e^4C_o\tau_o\bar{\phi}_o}{R^2}B &= \frac{8e^4C_o\tau_o\bar{\phi}_o}{R^2}\cdot\frac{1}{2\pi}\sqrt{\frac{b_oC_oR\sqrt{2m\gamma}}{\pi M}}\cdot\frac{\pi b_o^2z_o^2}{e}\cdot\frac{\pi R}{e^2N_e} \,, \\ &= 1/\pi \,,\end{aligned}$$

where equations (4.3) and (4.19) for the periods of the ions and electrons and the expression for N_e following equation (2.16) had been used in the simplification. The symbol ε in equation (4.26) is short for

$$\varepsilon = \left(\frac{e^2 N_i}{\pi b_o^2 z_o^2 R} - 1\right). \tag{4.27}$$

Since the derivation for n=even=2p+2 is exactly similar to the foregoing, we will omit it and just write down the final form of ζ_{2p+2} for p>0,

$$\begin{aligned}\zeta_{2p+2}(\phi,\bar{\phi},s) = {} & ((2p+2)\varepsilon-1)\,sc((2p+2),\phi)\cos(2p+2)\bar{\phi}/\bar{\phi}_o \\ & + \varepsilon\Big[\Big(\sum_{i=0}^{p-1}(2i+2)\,sc((2i+2),\phi)\Big)\cos(2p+2)\bar{\phi}/\bar{\phi}_o \\ & + (2p+2)\,sc((2p+2),\phi)\Big(\sum_{i=0}^{p}\cos 2i\bar{\phi}/\bar{\phi}_o - 1/2\Big)\Big].\end{aligned} \tag{4.28}$$

The ε of equation (4.27) was called $\hat{\varepsilon}$ in reference 27; and $\varepsilon=0$ corresponds to equation (2.21) which is the condition of no pile up of ions at the ends $\pm z_o$, while $\varepsilon>0$ corresponds to equation (2.22) which is the condition of pile up of ions at the ends.

5. Stability Analysis.

There are standard methods in solving general Fredholm equations,[34] but the actual solution of a particular problem is possible only if one is lucky enough to have a simple kernel. In the present case, the kernel as shown in equations (4.25-28) is degenerate which means the standard solution for a degenerate kernel is applicable here. But, it is also made up of an infinite sum with no obvious diminishing in the magnitude of the coefficients. This means that we have to deal with sum of n x n determinants, with n going to infinity, which is not easy to handle in general. However the difficult task of solving this equation can be avoided by making two simplifying observations.

First of all we rewrite the Fredholm (3.21) and its kernel as given by equations (4.25-28) for ease of reference

$$\hat{T}(\phi,s) = I[T;f_i] + \int_0^{\phi_o} d\phi''' \, K(\phi,\phi''',s)\hat{T}(\phi''',s), \qquad (5.1)$$

with

$$K(\phi,\phi''',s) = \sum_{n=1}^{\infty} \frac{n}{\pi(n^2+\bar{\tau}_o^2 s^2)} \zeta_n(\phi,\phi''',s),$$

for $n=2p+1$, $p \geq 0$,

$$\zeta_{2p+1}(\phi,\phi''',s)=((2p+1)\varepsilon-1)sc((2p+1),\phi)\cos(2p+1)\phi'''/\bar{\phi}_o$$
$$+\varepsilon[(\sum_{i=0}^{p-1}(2i+1)sc((2i+1),\phi))\cos(2p+1)\phi'''/\bar{\phi}_o$$
$$+(2p+1)sc((2p+1),\phi)(\sum_{i=0}^{p-1}\cos(2i+1)\phi'''/\bar{\phi}_o)],$$

for $n=2p+2$, $p>0$,

$$\zeta_{2p+2}(\phi,\phi''',s)=((2p+2)\varepsilon-1)sc((2p+2),\phi)\cos(2p+2)\phi'''/\bar{\phi}_o$$
$$+\varepsilon[(\sum_{i=0}^{p-1}(2i+2)sc((2i+2),\phi))\cos(2p+2)\phi'''/\bar{\phi}_o$$
$$+(2p+2)sc((2p+2),\phi)(\sum_{i=0}^{p}\cos 2i\phi'''/\bar{\phi}_o - 1/2)].$$

We notice that ϕ''' comes into the kernel through a cosine only. When these cosines get integrated over the interval $[0,\phi_o]$ with $\tilde{T}(\phi''',s)$ we get the cosine coefficients of the Fourier expansion of $\hat{T}$ over the said interval, and no more ϕ''' dependence on the rhs of equation (5.1). Thus, if we write the k^{th} cosine coefficient of $\hat{T}$ as

$$C_k(s) = \int_0^{\phi_o} d\phi\ \cos k\phi/\bar{\phi}_o \hat{T}(\phi,s), \qquad (5.2)$$

equation (5.1) is then

$$\hat{T}(\phi,s) = I[T,f_i] + \sum_{n=1}^{\infty} \frac{n}{\pi(n^2+\bar{\tau}_o^2 s^2)} j_n(\phi,s), \qquad (5.3)$$

where for $n=2p+1$, $p\geq 0$,

$$j_{2p+1}(\phi,s)=((2p+1)\varepsilon-1)sc((2p+1),\phi)C_{2p+1}(s)$$
$$+\varepsilon[(\sum_{i=0}^{p-1}(2i+1)sc((2i+1),\phi))C_{2p+1}(s)$$
$$+(2p+1)sc((2p+1),\phi)(\sum_{i=0}^{p-1}C_{2i+1}(s))], \qquad (5.4)$$

and for $n=2p+2$, $p>0$,

$$j_{2p+2}(\phi,s)=((2p+2)\varepsilon-1)sc((2p+2),\phi)C_{2p+2}(s)$$
$$+\varepsilon[(\sum_{i=0}^{p-1}(2i+2)sc((2i+2),\phi))C_{2p+2}(s)$$
$$+(2p+2)sc((2p+2),\phi)(\sum_{i=0}^{p}C_{2i}(s) - 1/2C_o(s))]. \qquad (5.5)$$

Each element in the sum on the rhs of (5.3) consists of terms proportional to

$$\sin k\phi/\phi_o C_i(s), \quad \cos k\phi/\bar{\phi}_o C_i(s),$$

which means that by integrating $(\cos k\phi/\bar{\phi}_o)$ x (5.3) over $[0,\phi_o]$ we pick up only the coefficients of $\cos k\phi/\bar{\phi}_o$ on the right, and get $C_k(s)$ on the left. By doing this for all $k=1,2,3,\ldots$ we get two uncoupled systems of linear equations in the odd and even cosine coefficients of $\hat{T}$. It turns out that the two systems are exactly equivalent in form, we will consider the odd system for illustration purpose, and quote the results from the even system when necessary. Hence, for the odd system we have

$$\begin{vmatrix} C_1 \\ C_3 \\ C_5 \\ \vdots \end{vmatrix} = \begin{vmatrix} I_1^c \\ I_3^c \\ I_5^c \\ \vdots \end{vmatrix} - \begin{vmatrix} \frac{1^2(1\varepsilon-1)}{u_1v_1} & \frac{3.1^2\varepsilon}{u_3v_1} & \frac{5.1^2\varepsilon}{u_5v_1} & \cdots \\ \frac{3^3\varepsilon}{u_3v_3} & \frac{3^2(3\varepsilon-1)}{u_3v_3} & \frac{5.3^2\varepsilon}{u_5v_3} & \cdots \\ \frac{5^3\varepsilon}{u_5v_5} & \frac{5^3\varepsilon}{u_5v_5} & \frac{5^2(5\varepsilon-1)}{u_5v_5} & \cdots \\ \vdots & \vdots & \vdots & \end{vmatrix} \begin{vmatrix} C_1 \\ C_3 \\ C_5 \\ \vdots \end{vmatrix} \tag{5.6}$$

where I^c_{2p+1} came from integrating the inhomogeneous term over $[0,\phi_o]$, and

$$u_k = k^2 + \bar{\tau}_o^2 s^2, \tag{5.7}$$

$$v_k = k^2 + \bar{\phi}_o^2 s^2. \tag{5.8}$$

The diagonal elements in the above matrix were obtained from the (2p+1)th terms in the sum of (5.3). Each one of them came from integrating the first term in (5.4) over $[0,\phi_o]$,

$$\frac{(2p+1)((2p+1)\varepsilon-1)}{\pi u_{2p+1}} \int_0^{\phi_o} d\phi \; sc((2p+1),\phi)\cos(2p+1)\phi/\bar{\phi}_o$$

$$= -\frac{(2p+1)^2((2p+1)\varepsilon-1)}{\pi\bar{\phi}_o u_{2p+1}v_{2p+1}} \int_0^{\phi_o} d\phi \; \cos^2(2p+1)\phi/\bar{\phi}_o,$$

$$= -\frac{(2p+1)^2((2p+1)\varepsilon-1)}{u_{2p+1}v_{2p+1}}.$$

The (2p+1)th below row elements came from the same (2p+1)th term in the sum of (5.3). They were obtained by integrating the third term in (5.4)

$$\frac{(2p+1)^2\varepsilon}{\pi u_{2p+1}}\int_0^{\phi_0} d\phi\ sc((2p+1),\phi)\cos(2p+1)\phi/\bar{\phi}_0 = -\frac{(2p+1)^3\varepsilon}{u_{2p+1}v_{2p+1}}.$$

And, finally, the above diagonal elements were picked up by $\cos(2p+1)\phi/\bar{\phi}_0$ from the (2q+1)th, q>p, term in the sum of (5.3)

$$\frac{(2q+1)\varepsilon}{\pi u_{2q+1}}\sum_{i=0}^{q-1}(2i+1)\int_0^{\phi_0} d\phi\ sc((2i+1),\phi)\cos(2p+1)\phi/\bar{\phi}_0$$

$$= -\frac{(2q+1)(2p+1)^2\varepsilon}{\pi\bar{\phi}_0 u_{2q+1}v_{2p+1}}\int_0^{\phi_0} d\phi\ \cos^2(2p+1)\phi/\bar{\phi}_0$$

$$= -\frac{(2q+1)(2p+1)^2\varepsilon}{u_{2q+1}v_{2p+1}}.$$

The Fourier sine coefficients of $\hat{T}(\phi,s)$,

$$S_k(s) = \int_0^{\phi_0} d\phi\ \hat{T}(\phi,s)\sin k\phi/\bar{\phi}_0, \qquad (5.9)$$

are readily obtained from the cosine coefficients. For, if we integrate $(\sin(2p+1)\phi/\bar{\phi}_0)$ x (5.3) over $[0,\phi_0]$, we get

$$S_{2p+1}(s) = I^s_{2p+1} + s\bar{\phi}_0\Big[\frac{(2p+1)^2\varepsilon}{u_{2p+1}v_{2p+1}}\sum_{i=0}^{p-1} C_{2i+1}(s)$$

$$+ \frac{(2p+1)((2p+1)\varepsilon-1)}{u_{2p+1}v_{2p+1}} C_{2p+1}(s)$$

$$+ \frac{(2p+1)\varepsilon}{v_{2p+1}}\sum_{i=p+1}^{\infty} \frac{(2i+1)}{u_{2i+1}} C_{2i+1}(s)\Big], \qquad (5.10)$$

which is just a sum of the Fourier cosine coefficients and the inhomogeneous term. Hence, if we can solve the system (5.6) and a similar system in the even cosine coefficients, we know all about $\hat{T}$ in terms of its Fourier components.

Solving linear equations is always easier than that of Fredholm equations. However we do not even have to do this easier problem. Because, as was observed by Ehrman,[12] the quantity of direct physical interest is not $\hat{T}(\phi,s)$ but is its inverse Laplace transform

$$T(\phi,t) = \frac{1}{2\pi i}\int_{a-i\infty}^{a+i\infty} ds\, e^{st}\hat{T}(\phi,s),$$

where the integral runs parallel to the imaginary axis, and $a>0$ is large enough so that no singularity of $\hat{T}(\phi,s)$ has real part greater than a. In applying this inversion formula for $t>0$, we have to displace the contour leftwards, indenting it so as to capture any singularities of $\hat{T}(\phi,s)$. If they are all poles, then $T(\phi,t)$ will be a sum of terms proportional to $\exp(s_k t)$, where $s_1, s_2, \ldots$ are the poles of

$\hat{T}(\phi,s)$. If there is an s_k with a real part greater than zero, then our system is unstable; if otherwise, it is stable.

Since all the informations of $\hat{T}(\phi,s)$ is contained in its Fourier sine and cosine coefficients, all we have to do is to consider the singularities of these quantities. From equations (5.10), the singularities of the sine coefficients are those of the cosine coefficients and the eigenfrequencies

$$u_k = k^2 + \bar{\tau}_0^2 s^2 = 0, \tag{5.11}$$

$$v_k = k^2 + \bar{\phi}_0^2 s^2 = 0. \tag{5.12}$$

Since the cosine coefficients are obtained by solving the linear system (5.6) and a similar system for the even coefficients, their singularities are the zeros of the determinant of the coefficients, which is given by

$$\begin{vmatrix}
\left(1+\dfrac{1^2(1\varepsilon-1)}{u_1v_1}\right) & \dfrac{3.1^2\varepsilon}{u_3v_1} & \dfrac{5.1^2\varepsilon}{u_5v_1} & \dfrac{7.1^2\varepsilon}{u_7v_1} & \cdots \\
\dfrac{3^3\varepsilon}{u_3v_3} & \left(1+\dfrac{3^2(3\varepsilon-1)}{u_3v_3}\right) & \dfrac{5.3^2\varepsilon}{u_5v_3} & \dfrac{7.3^2\varepsilon}{u_7v_3} & \cdots \\
\dfrac{5^3\varepsilon}{u_5v_5} & \dfrac{5^3\varepsilon}{u_5v_5} & \left(1+\dfrac{5^2(5\varepsilon-1)}{u_5v_5}\right) & \dfrac{7.5^2\varepsilon}{u_7v_5} & \cdots \\
\dfrac{7^3\varepsilon}{u_7v_7} & \dfrac{7^3\varepsilon}{u_7v_7} & \dfrac{7^3\varepsilon}{u_7v_7} & \left(1+\dfrac{7^2(7\varepsilon-1)}{u_7v_7}\right) & \cdots \\
\vdots & \vdots & \vdots & \vdots &
\end{vmatrix} \tag{5.13}$$

and a similar one for the even system.

We consider the easy case first, that is when equation (2.21) holds, and from equation (4.27) this is the case when $\varepsilon=0$. The determinant in (5.13) is then just an infinite product

$$\prod_{n=1}^{\infty} \left(1- \frac{n^2}{u_n v_n}\right),$$

where we have included factors from the even coefficients also. The zeros of this infinite product is just the zeros of each factor

$$(u_n v_n - n^2) = 0,$$

From equation (5.7,8), this is

$$(n^2+\bar{\tau}_o^2 s^2)(n^2+\bar{\phi}_o^2 s^2) - n^2 = 0,$$

or,

$$s^2 = \frac{n^2}{2}\left[\left(\frac{1}{\bar{\tau}_o^2}+\frac{1}{\bar{\phi}_o^2}\right) \pm \sqrt{\left(\frac{1}{\bar{\tau}_o^2}+\frac{1}{\bar{\phi}_o^2}\right)^2 - \frac{4}{\bar{\tau}_o^2\bar{\phi}_o^2}\left(1-\frac{1}{n^2}\right)}\right]. \qquad (5.14)$$

Since we require $\mathrm{Re}(s)\leq 0$ for stability, the only way for (5.14) to satisfy this condition is to have s^2 real and negative, so that $\mathrm{Re}(s)=0$. Translating this requirement into (5.14) we want the discriminant to lie in between the limits

$$0 \leq \left(\frac{1}{\bar{\tau}_o^2} + \frac{1}{\bar{\phi}_o^2}\right)^2 - \frac{4}{\bar{\tau}_o^2 \bar{\phi}_o^2}\left(1 - \frac{1}{n^2}\right) < \left(\frac{1}{\bar{\tau}_o^2} + \frac{1}{\bar{\phi}_o^2}\right)^2 .$$

The left hand inequality guarantees the radical is real, and the right hand one guarantees the square bracket in (5.14) is positive. To see that both of these inequalities are satisfied is trivial. For the left hand one, we rewrite the discriminant as

$$\left(\frac{1}{\bar{\tau}_o^2} - \frac{1}{\bar{\phi}_o^2}\right)^2 + \frac{4}{\bar{\tau}_o^2 \bar{\phi}_o^2 n^2},$$

which is positive for all n. For the right hand one, we rewrite the inequality as

$$-\frac{4}{\bar{\tau}_o^2 \bar{\phi}_o^2}\left(1 - \frac{1}{n^2}\right) < 0.$$

This is always satisfied as the factor

$$(1 - 1/n^2) \geq 0,$$

for all $n>0$. Hence for the case when equation (2.21) holds our system is always stable.

For the case when equation (2.22) holds, we have $\varepsilon>0$, and all the elements in (5.13) must be reckoned with. A necessary and sufficient condition for an infinite linear system of equations to have a solution was given by Bôcher and Brand[35] but its application requires a known inhomo-

geneous term in equation (5.6). We assume that for physically possible perturbations a solution does exist, and can be found by the method of reduction. That is we truncate (5.6) at a finite N and form determinants

Δ_N = determinant of coefficients of C_k,

$\Delta_N^{(k)}$ = determinant formed from Δ_N with the k^{th} column replaced by the inhomogeneous term.

By taking succeeding larger N's, if both of them tend to a limit

$$\lim_{N\to\infty} \Delta_N = \Delta,$$

$$\lim_{N\to\infty} \Delta_N^{(k)} = \Delta^{(k)},$$

the solution is given by

$$C_k = \Delta^{(k)}/\Delta.$$

Since we are only interested in the zeros of Δ, we will apply the method of reduction to (5.13) only.

For the purpose of numerical calculation which we will be using, we apply the usual rules in finite determinants to transform (5.13) into .

$$\frac{1^4\varepsilon\ 3^4\varepsilon\ 5^4\varepsilon}{u_1v_1u_3^2v_3u_5^2v_5}\cdots \begin{vmatrix} d_1 & u_1 & u_1 & u_1 & \cdots \\ 1 & d_3u_3 & u_3/3 & u_3/3 & \cdots \\ 1 & u_3/3 & d_5u_5 & u_5/5 & \cdots \\ 1 & u_3/3 & u_5/5 & d_7u_7 & \cdots \\ \vdots & \vdots & \vdots & \vdots & \\ \vdots & \vdots & \vdots & \vdots & \\ \vdots & \vdots & \vdots & \ddots & \end{vmatrix} \qquad (5.15)$$

where

$$d_k = (u_kv_k + k^2(k\varepsilon-1))/k^4\varepsilon. \qquad (5.16)$$

There are three parameters, $\bar{\tau}_0^2$, $\bar{\phi}_0^2$ and ε in (5.15), and they can be reduced to two if we define

$$r^2 = \bar{\tau}_0^2 s^2,$$
$$y = \bar{\tau}_0^2/\bar{\phi}_0^2.$$

We can now proceed to find the zeros of (5.15) in the complex r^2-plane for parameters ε, $y>0$.

Truncating the infinite determinant in (5.15) at N=3, 5,...,2n-1,... we get determinants of order 2,3,4,...,n+1,... Expanding these truncated determinants in the usual manner we obtain polynomials of degree 5,8,11,...,3n+2,... in r^2. For example, truncating at N=3 we get $d_1d_3u_3-u_1$, a polynomial of degree 5 in r^2. Of the two terms in this polynomial, the first is 4 degrees higher than the second one. This is true for all higher orders of truncation , that is the term consisting of the

the product of the diagonal elements in (5.15) is of 4 degrees higher than the rest. It would be nice if we could take the diagonal product as an approximation for our determinant. Unfortunately it is the roots that we are looking for, and they can depend quite sensitively on the lower order terms. However, after detailed numerical calculation we find that in the region we are most interested in, the roots from the diagonal product agree quite well with those of the full determinant; and where they disagree. the diagonal roots serve as an indicator as to the behaviour of the roots of the full determinants would behave as higher orders of truncation are taken.

Because of their importance as an indicator, we take a look at the roots of the diagonal product, $d_1(d_3u_3)(d_5u_5)\ldots$ first. They are the eigenfrequencies $s^2=-k^2/\bar{\tau}_0^2$, and the roots of d_k, k=odd. Since each of the d_k's is a quadratic in r^2, the roots for r^2 are easily found to be

$$r_{kl} = -(k^2/2)[(1+y)-\sqrt{D_k(\varepsilon,y)}], \qquad (5.17)$$

$$r_{ks} = -(k^2/2)[(1+y)+\sqrt{D_k(\varepsilon,y)}], \qquad (5.18)$$

where

$$D_k(\varepsilon,y) = (1+y)^2-4y\left(1+\frac{k\varepsilon-1}{k^2}\right), \qquad (5.19)$$

and the subscripts kl, ks stand for the algebraic larger

and smaller roots whenever they are real. The region of parameter space (ε,y) where $r_{kl,s}$ take non-real values is of course bounded by the curve $D_k(\varepsilon,y)=0$. For each k we solve for ε,

$$\varepsilon = k\frac{(1-y)^2}{4y} \pm \frac{1}{k}. \qquad (5.20)$$

It has the form shown in fig. 5 below.

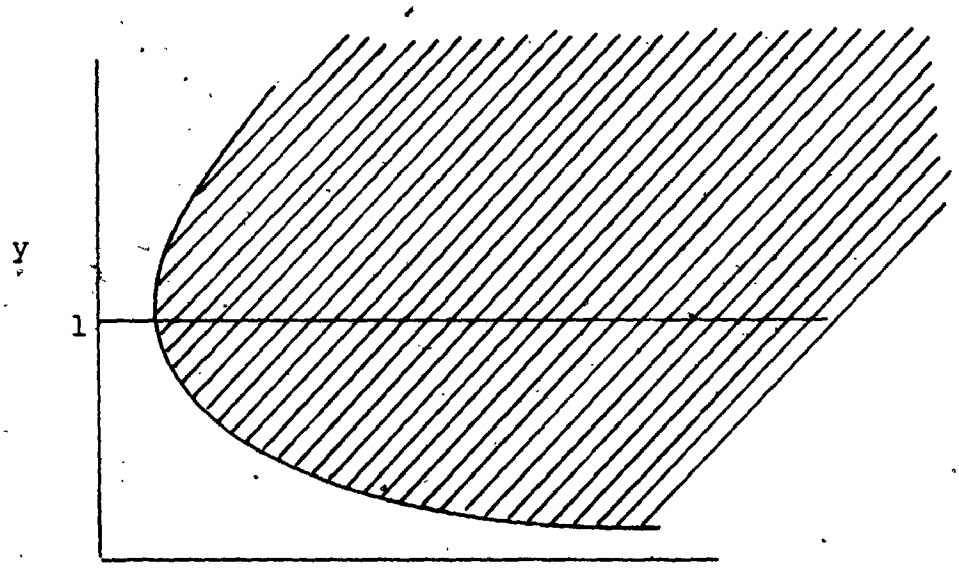

fig. 5 Region of (ε,y) plane where d_k has non-real roots in r^2.

Since we are only interested in the positive values of ε and y, the plot only shows this part of $D_k=0$. The hatched region to the right of the curve has $D_k<0$, and hence gives rise to non-zero imaginary part to $r_{kl,s}$. To the left of this curve they are real. A detailed plot for k=1,3,5,7 and 9 is shown in fig. 6 (From this number on, all figures are numerical plots, and are placed at the end of this

section). There, the D_k curves displayed a tendency to approaches the line y=1 as k increases. This can be seen analytically by calculating the width of each D_k curve at $\varepsilon=\varepsilon_0(\varepsilon_0>1$, to include all the curves $D_k=0$). Setting $\varepsilon=\varepsilon_0$ in equation (5.20) we get

$$(\text{width of } D_k \text{ curve at } \varepsilon=\varepsilon_0)=4\left[\frac{1}{k}\left(\varepsilon_0-\frac{1}{k}\right)+\frac{1}{k^2}\left(\varepsilon_0-\frac{1}{k}\right)^2\right]^{1/2},$$

which is a decreasing function of k for k>1, $\varepsilon_0>1.5$ (This value is obtained from fig. 6, rather than considering the derivative of the above equation). The tip of each D_k curve lies on the line y=1, and approaches the y axis as 1/k, as can be seen from the same equation (5.20) by putting y=1.

We also find it useful to show graphically the variation of the roots $r_{kl,s}$ with respect to y for fixed values of ε. This is shown in fig. 7 for k=5. It is observed that when $0<\varepsilon<1/k$ (=.2 for the present case), $r_{kl,s}$ are real; when $\varepsilon>1/k$, they are complex ('complex' shall be taken to mean 'having a non-zero imaginary part') for a certain range in the neighborhood of y=1; and for all $\varepsilon>0$, $\mathrm{Re}(r_{kl,s})<0$. Since ε must be positive fig. 7 shows that all values of $\mathrm{Re}(r_{kl,s})$ are bounded by the curves with $\varepsilon=0$. This is shown in fig. 8, for k=1,3,5,7 and 9.

Let us now consider the roots of the full determinants. Numerical calculations show that starting from the 5 roots for r^2 at N=3, each higher order of truncation contains all the roots of the preceding one, and brings in three more roots. Table 1 shows the roots for each order of truncation with ϵ=1.25 and y=.3.

3	5	7	9
-.37	-.36	-.36	-.36
-.88	-.89	-.89	-.89
-4.47	-3.92	-3.86	-3.84
-7.12	-7.68	-7.69	-7.69
-9.15	-9.15	-9.15	-9.15
	-10.52	-9.45	-9.33
	-21.26	-20.68	-18.75
		±i2.28	-21.19
	-25.71	-25.71	-25.71
			-32.57
		-43.22	-41.98
		-50.51	-50.51
			-73.02
			-83.51

Table 1. Roots of determinants truncated at N=3,5,7 and 9. The 7th and 8th roots of N=7 are complex.

The roots in most of the rows show a clear trend of convergence as higher orders of truncation are taken. The real parts of all roots of r^2 are negative.

If we order the roots according to the size of their real parts, then there appear to be some regular pattern in the region y<1. It should be noted that, since the polynomials we are dealing with have real coefficients, complex roots appear as pairs of complex conjugates only. The ordering within each pair of conjugates is not important,

the essential thing is to have them placed in the j^{th} and $(j+1)^{th}$ position as their real part dictates.

This method of ordering delineates the complex roots in this region into two groups. Roughly speaking, the distinction between them lies in the complexity of the diagonal roots. In the first group the complex roots can be considered as approximate values of the diagonal roots which are complex; whereas in group 2, the diagonal roots are actually real. There are exceptions to the rules just stated for ε sufficiently large, but we shall give better methods of defining these two groups in what follows.

The group 1 complex roots are shown in fig. 9a, b, c and d for determinants truncated at N=3,5,7 and 9 respectively. The curves shown in these figures mark off (ε,y) values where the j^{th} and $(j+1)^{th}$ roots are complex, that is, any point to the left of the (j,j+1) curve has real j^{th} and $(j+1)^{th}$ roots; if otherwise, they are complex. These figures show that starting from N=3 with only (1,2) and (3,4) curves, one new curve is added onto the previous one for each higher order of truncation, and that the region defined by any (j,j+1) curve do not differ by an appreciable amount in the region $y<1$.

Comparing the $y<1$ part of fig. 6 with that of fig. 9d for the case of N=9, it was observed that the D_k

curves match closely with the (j,j+1) curves. Thus, we can identify the complex roots from d_1 of the diagonal as the 'source' of the (1,2) complex pair in the full determinant. Likewise, the complex roots for d_3, d_5, d_7 and d_9 of the diagonal can be identified as the "source" of the (3,4), (6,7), (9,10) and (12,13) pairs in the full determinant. A comparison of the diagonal roots and the roots of the full determinant for the following values of (ε,y) in table 2 shows that the diagonal roots are quite good an approximation here.

ε=1. y=.6		ε=.6 y=.8		ε=.4 y=1.	
N=9	diag	N=9	diag	N=9	diag
-.52	-.60	-.30	-.32	-.21	-.22
-1.00	-1.00	-1.45	-1.47	-1.75	-1.77
-6.89 ±i2.59	-7.20 ±i2.75	-7.80 ±i2.23	-8.10 ±i2.23	-8.57 ±i1.50	-9.00 ±i1.34
-9.28	-9.00	-9.34	-9.00	-9.65	-9.00
-19.26 ±i5.76	-20.00 ±i5.92	-21.64 ±i6.02	-22.50 ±i5.81	-23.91 ±i5.32	-25.00 ±i5.00
-26.35	-25.00	-26.45	-25.00	-26.87	-25.00
-38.37 ±i8.85	-39.20 ±i8.96	-42.66 ±i10.68	-44.10 ±i10.07	-46.97 ±i10.07	-49.00 ±i9.39
-51.92	-49.00	-52.12	-49.00	-52.93	-49.00
-62.00 ±i16.49	-64.80 ±i11.24	-70.44 ±i17.95	-72.90 ±i14.82	-77.99 ±i16.71	-81.00 ±i14.51
-85.90	-81.00	-86.26	-81.00	-81.70	-81.00

Table 2. Comparison of the diagonal roots and the roots of the determinant truncated at N=9.

Since this group of complex roots is due to the fact that the diagonal roots are complex, then from what was said on the diagonal roots, we expect that as higher orders of truncation are taken, the full determinant will have complex roots right up to $\varepsilon=0$ at $y=1$. On the other hand, the lowest y value in the region $\varepsilon>1$ where group I complex roots can appear is defined by the (1,2) curve, as all other curves obtained from the higher orders of truncation lie above it.

The roots given in the above table are actually in the complex plane $r^2=\bar{\tau}_0^2 s^2$, therefore the growth rate is obtained by taking the imaginary part of the square root of each unstable mode and divide by $\bar{\tau}_0$, that is,

$$\text{growth rate} = \mathrm{Re}\sqrt{\bar{\tau}_0^2 s^2}/\bar{\tau}_0.$$

Since τ_0 and ϕ_0 are the characteristic times here we want to compare the growth rate with one of these periods. Since τ_0 is the shorter period in this region $y<1$, we compare the growth rate with τ_0. That is we want the ratio

$$\rho = \frac{(\text{growth rate})^{-1}}{\tau_0} = \frac{1}{2\pi\,\mathrm{Re}\sqrt{\bar{\tau}_0^2 s^2}}, \qquad (5.21)$$

and consider the unstable mode to harmless if $\rho>10$. This ratio is calculated for all the unstable modes in table 2, and listed in the following table.

.33	.41	.63
.25	.25	.30
.22	.20	.22
.15	.15	.17

Table 3. ρ of the unstable modes in table 2.

Clearly, none of these modes is tolerable. Furthermore, for a fixed y, the growth rate in this group increases as ε increases, hence this region must be avoided.

If we look at the asymptote as $\varepsilon \to \infty$ of the lower branch of each curve in fig. 6 and 9 more closely, we find that the (j,j+1) curves are squeezed together as compared with those of the $D_k=0$ curves. In fact if the D_k curves were continued on, each one of them would approach the axis as $k^2/4(k\varepsilon-1)$. However, for the (j,j+1) curves they become parallel to the ε axis at some finite y values above it. Below these curves, this group of complex pairs give way to the group 2 complex pairs we had mentioned before.

This second group is shown in fig. 10a, b, c and d. As in the previous case, any higher order of truncation contains all the complex pairs of its predecessors while adding some new ones of its own. We have chosen the cut off of the curves at $\varepsilon=2$ for clarity of presentation. If the curves in fig. 10d were to continue beyond $\varepsilon=2$, they would criss-cross each other making identification of the

boundary of each complex pair very difficult. On the other hand, the trend as how each curve will go beyond $\varepsilon=2$ is clear: they will all touch the ε axis at some large values of ε. This is shown for the (2,3) curve of N=3 at the upper right of fig. 10a.

ε	7th & 8th roots of the full det.		r_{71} & r_{5s} of the diag.	
	7th	8th	r_{71}	r_{5s}
.05	-21.99	-24.98	-21.99	-25.61
.10	-22.29	-24.91	-22.29	-25.41
.15	-22.60	-24.76	-22.58	-25.21
.20	-22.92	-24.54	-22.89	-25.00
.25	-23.30	-24.24	-23.19	-24.78
.30	-23.81 ±i.31		-23.51	-24.56
.35	-23.84 ±i.53		-23.84	-24.33
.40	-23.86 ±i.57		-24.17	-24.09
.45	-23.89 ±i.45		-24.52	-23.83
.50	-23.63	-24.19	-24.88	-23.57
.55	-23.19	-24.67	-25.24	-23.29
.60	-22.85	-25.04	-25.63	-23.00
.65	-22.52	-25.52	-26.02	-22.69

Table 4. A comparison of the 7th and 8th roots of the determinant truncated at N=9 to r_{71} and r_{5s} of the diagonal roots.

In order to understand the behaviour of this group, we compare the 7th and 8th roots of the determinant truncated at N=9 with the roots r_{71} and r_{5s} of the diagonal for y=.46 and ε as specified in table 4. We observe that r_{71} starts out at a value less negative than r_{5s}, then it becomes increasingly negative while r_{5s} goes the other way as ε increases, so that finally one passes the other at some ε_0, $.35<\varepsilon_0<.40$. In the full determinant the 7th and 8th

roots start out with approximately the values of r_{71} and r_{5s} when $\varepsilon<\varepsilon_0$ and when they are not close to each other. Near ε_0, $|r_{71}-r_{5s}|\leq 1$, the relatively smaller values of the off diagonal terms in the full determinant are big enough to push this neighboring pair of roots away from the real axis. When $\varepsilon>\varepsilon_0$ the diagonal roots are far apart, and the corresponding roots of the full determinant are real again.

			ε_i	γ	ρ_m
a. when r_{31} overtakes r_{ks}, $k<3$.	(r_{31},r_{1s})	(2,3)	1.5	.08	---
b. when r_{51} overtakes r_{ks}, $k<5$.	(r_{51},r_{3s}) (r_{51},r_{1s})	(4,5) ---	.2 3.3	.36 .02	2.24 ---
c. when r_{71} overtakes r_{ks}, $k<7$.	(r_{71},r_{5s}) (r_{71},r_{3s}) (r_{71},r_{1s})	(7,8) (5,6) ---	.1 .2 (>5.)	.52 .16 ---	.83 9. ---
d. when r_{91} overtakes r_{ks}, $k<9$.	(r_{91},r_{7s}) (r_{91},r_{5s}) (r_{91},r_{3s}) (r_{91},r_{1s})	(10,11) (8,9) (6,7) ---	.1 .2 .7 (>5.)	.62 .30 .10 ---	.37 1.60 20. ---

Table 5. Group 2 complex pairs in the region $\gamma<1$. The values of the rightmost three columns are all obtained from the determinant truncated at N=9. In the typewriter used for the above table, both the letter 'l' and the number '1' are from the same key, but one should be able to distinguish them from context.

By doing the same thing with the other pairs in this group, we find that they follow the similar pattern as the (7,8) pair. Depending on which two of the diagonal roots are passing each other the complex pairs in this group

can be divided into the subgroups shown in table 5. Hence, if it is possible to locate all the places where a r_{il} root overtakes a r_{js} $(i>j)$ root as ε increases, we can account for all the complex pairs of this group. This can be done by looking at fig. 8. The region bounded by r_{il}, r_{js} $(\varepsilon=0, i>j)$ curves and the vertical axis is where overtaking of one root by the other is possible. The correspondence of this region to the group 2 complex pairs in the full determinant is further confirmed by the fact that the y values of each intersection in fig. 8 are approximately the y values in fig. 10d where their corresponding complex pairs start. The latter is given by the 5th column in table 5. The slight discrepancy is consistent in these two sets of y values, in that those y values of column 5 in table 5 are a little less than that of fig. 8. If we look at the imaginary parts of the roots in any of the subgroups, we find that they increase as y decreases. It is possible that due to the limitation on the accuracy of our computer program we might have missed some of the very small complex parts. However this is not going to affect our main argument, because the program used can pick up complex parts as small as 10^{-3} in r^2, which, depending on the size of the real part of r^2, give rise to a ρ of the order at least 10^3. We can neglect these modes.

ε_i of column 4 is the ε value when a complex pair

first occur. We have tried to find the complex pairs cause by the crossing of (r_{71}, r_{1s}) and (r_{91}, r_{1s}) up to $\varepsilon=5.$, but have not been able to do so. We may have missed them, or they may have started at beyond $\varepsilon=5$. In any case their non-appearance do not affect our argument, because it will be shown later that if they do exist at all they must have very small growth rates. The ε_i values of column 4 are obtained from fig. 10d. We see that within each subgroup ε_i of each pair moves to the right as we go down the subgroup. This means that if higher orders of truncation are taken, the new complex pairs they contribute will start from either higher y or ε values, leaving the patch $y<.1$, $\varepsilon<.6$ stable.

If we look at column 6 in table 5, we can be more optimistic in choosing the stable patch. For, here we have calculated ρ_m, the ρ for maximum observed growth rate for each complex pair with $\varepsilon<1$. As we go down each of the subgroup c and d, ρ_m increases. The last observed ρ_m in d is already 20, which can be considered harmless. Since the complex pairs from (r_{71}, r_{3s}) and (r_{91}, r_{3s}) have $\rho_m=9$, and 20 respectively, if the pairs (r_{71}, r_{1s}) and (r_{91}, r_{1s}) mentioned in the preceeding paragraph do exist, they can have only larger ρ_m. As for the higher orders of truncation, we expect the first few pairs in the new subgroup they introduce will have large growth rates, but they also have

higher y values. The rest of these new pairs will have either very small growth rates or are pushed to the right. Thus, for the odd system, we can consider the hatched corner in fig. 10d to be stable, as any of the new complex pairs due to higher orders of truncation will not intrude into this region.

The relative simple pattern of the region $y<1$ is almost completely lost when we go over to $y>1$. First of all the (1,2), (3,4), (6,7), (9,10) and (12,13) complex pairs are not confined to approximately the same position in (ε,y) plane when d_1, d_3, d_5, d_7 and d_9 of the diagonal have complex roots. In fact, as can be seen from fig. 9d they cover a much wider region in the (ε,y) plane. Secondly, the other group of complex pairs do not have similar behaviour as their counter parts in $y<1$. There, it was an easy matter to recognize a correspondence of the crossing of $(r_{i1},r_j s)$ diagonal roots to the complex pair in the full determinant. Whereas here, no such clear cut correspondence can be made.

The only pattern remaining seems to be the containment of the complex pairs in a lower order of truncation by that of a higher order. It may be possible to find some recognizable pattern in this region, but it is not necessary to do so. For, as we increase y only a few complex pairs emerge beyond y=100. They are shown in fig. 11.

In this figure we have plotted each curve up to y=200, but investigation up to y=400 show they run almost parallel to the axis. Since the ratio of ion to electron period cannot be too big, calculation beyond y=400 ($\bar{\tau}_o/\bar{\phi}_o$=20) was discontinued.

It is rather interesting to observe that as y becomes large, the real parts of these complex pairs approaches the even eigenfrequencies, that is -4^2, -6^2, and -8^2. As the truncation at N=5 produces only one (3,4) pair, truncation at N=7 produces (3,4) and (5,6) pairs, and that of N=9 adds (7,8) on top of the previous pairs; one is forced to conclude that if higher orders are included, more complex pairs with their real parts -10^2, -12^2, ... will appear. From fig. 11, they will finally crowd down to ε=0 making this region completely unstable.

Consideration of the growth rates of the unstable modes contributed by these complex pairs is not going to be of help. Since ϕ_o is the shorter period in this region, we want the ratio

$$\rho_e = \frac{(\text{growth rate})^{-1}}{\phi_o} = \rho\sqrt{y},$$

instead of ρ. Tables 6a and b show some of the ρ_e's at y=60 and 300. Only the growth rate of the (3,4) pair at ε=.90 y=300 is small enough to give a ρ_e>10. And for the same

value of ε, the (7,8) pair has the largest growth rate, diminishing down to the (3,4) pair. This shows that if new pairs are obtained from an higher order of truncation, their growth rates will be even more dangerous.

a. y=60

ε	(3,4)	(5,6)	(7,8)
.30			4.57
.40			2.94
.50			2.33
.60		7.36	2.02
.70		2.94	1.78
.80		2.25	1.63
.90	6.45	1.86	1.47
1.00	3.26	1.63	1.40

b. y=300

ε	(3,4)	(5,6)	(7,8)
.80		7.80	4.85
.90		5.54	4.16
1.00	11.70	4.50	3.64

Table 6. Some ρ_e values of the pairs that extend beyond y=100.

The even system corresponding to (5.6) is given by

$$\begin{pmatrix} C_2 \\ C_4 \\ C_6 \\ \vdots \end{pmatrix} = \begin{pmatrix} I_2^c \\ I_4^c \\ I_6^c \\ \vdots \end{pmatrix} - \begin{vmatrix} \frac{2^2(2\varepsilon-1)}{u_2v_2} & \frac{4.2^2\varepsilon}{u_4v_2} & \frac{6.2^2\varepsilon}{u_6v_2} & \cdots \\ \frac{4^3\varepsilon}{u_4v_4} & \frac{4^2(4\varepsilon-1)}{u_4v_4} & \frac{6.4^2\varepsilon}{u_6v_4} & \cdots \\ \frac{6^3\varepsilon}{u_6v_6} & \frac{6^3\varepsilon}{u_6v_6} & \frac{6^2(6\varepsilon-1)}{u_6v_6} & \cdots \\ \vdots & \vdots & \vdots & \end{vmatrix} \begin{pmatrix} C_2 \\ C_4 \\ C_6 \\ \vdots \end{pmatrix}$$

Due to the fact that the zeroth term of (4.9) is zero

$$\xi_0 = g_0 h_0 = 0,$$

the zeroth Fourier coefficient must be zero also. If we follow through the derivations in sections 4 to 5, $\xi_0=0$ implies that $\eta_0=\zeta_0=j_0=0$, which in turn implies that $C_0=I_0$ when we take the Fourier coefficients of equation (5.2). This means that C_0 (The zeroth Fourier coefficient, not the constant in f_e of equation (2.13)) depends on the initial perturbation only. Since a non-zero C_0 implies a uniform stretching or compressing of the water bag which is contrary to the incompressibility conclusion of Liouville's theorem, we must have $I_0=0$ for a physical perturbation. Hence, $C_0=0$.

Exactly similar behaviour is shown by the above even system as the odd system (5.6). To avoid repetition we merely include all the corresponding curves for the

even system. The curve corresponding to fig. 7 was omitted as it serves is equally useful for both the odd and the even diagonal roots. The stable patch for the even system is shown in fig. 15d, therefore the entire system is stable in the intersection of the two patches in fig. 10d and fig. 15d.

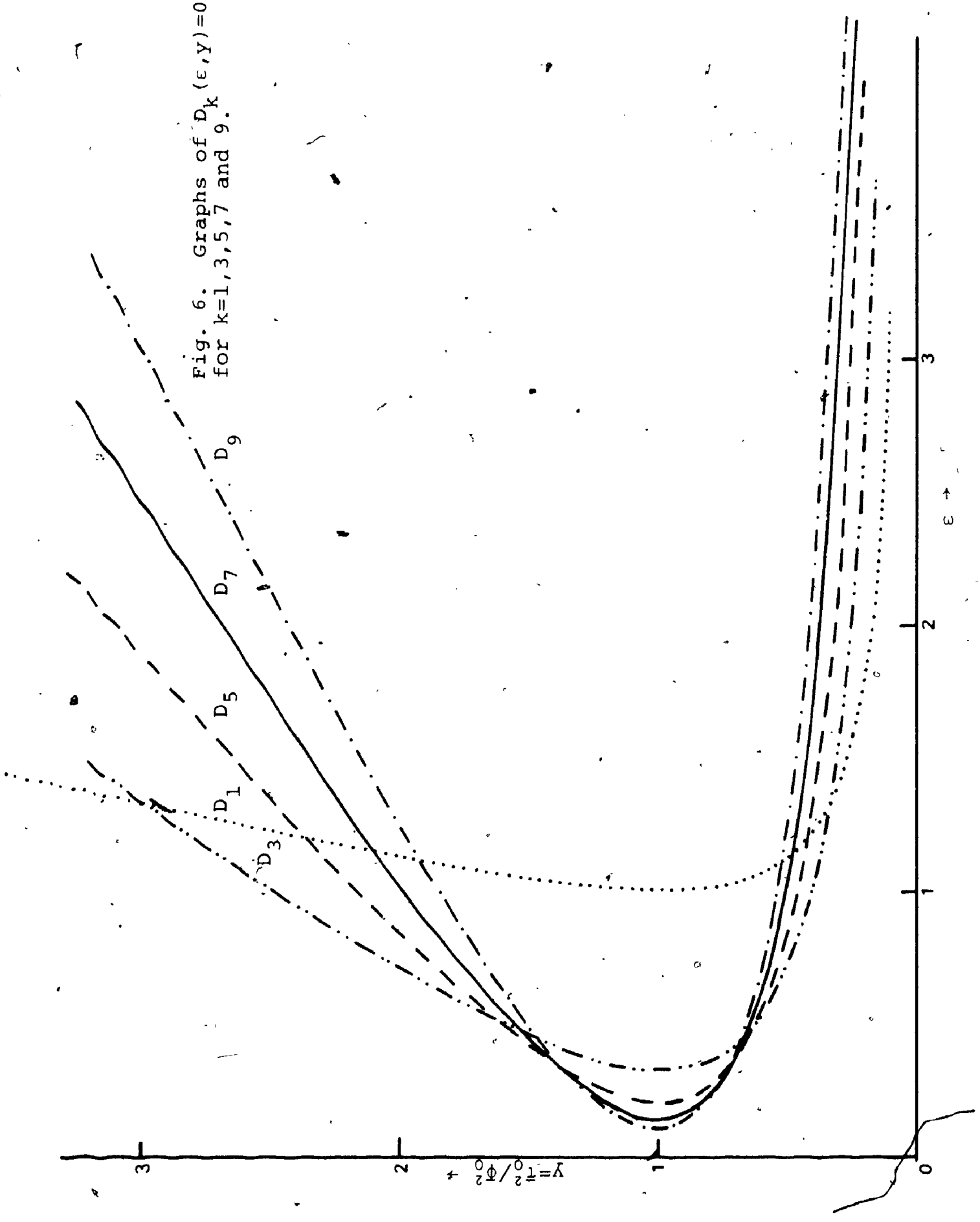

Fig. 6. Graphs of $D_k(\epsilon, y)=0$ for k=1,3,5,7 and 9.

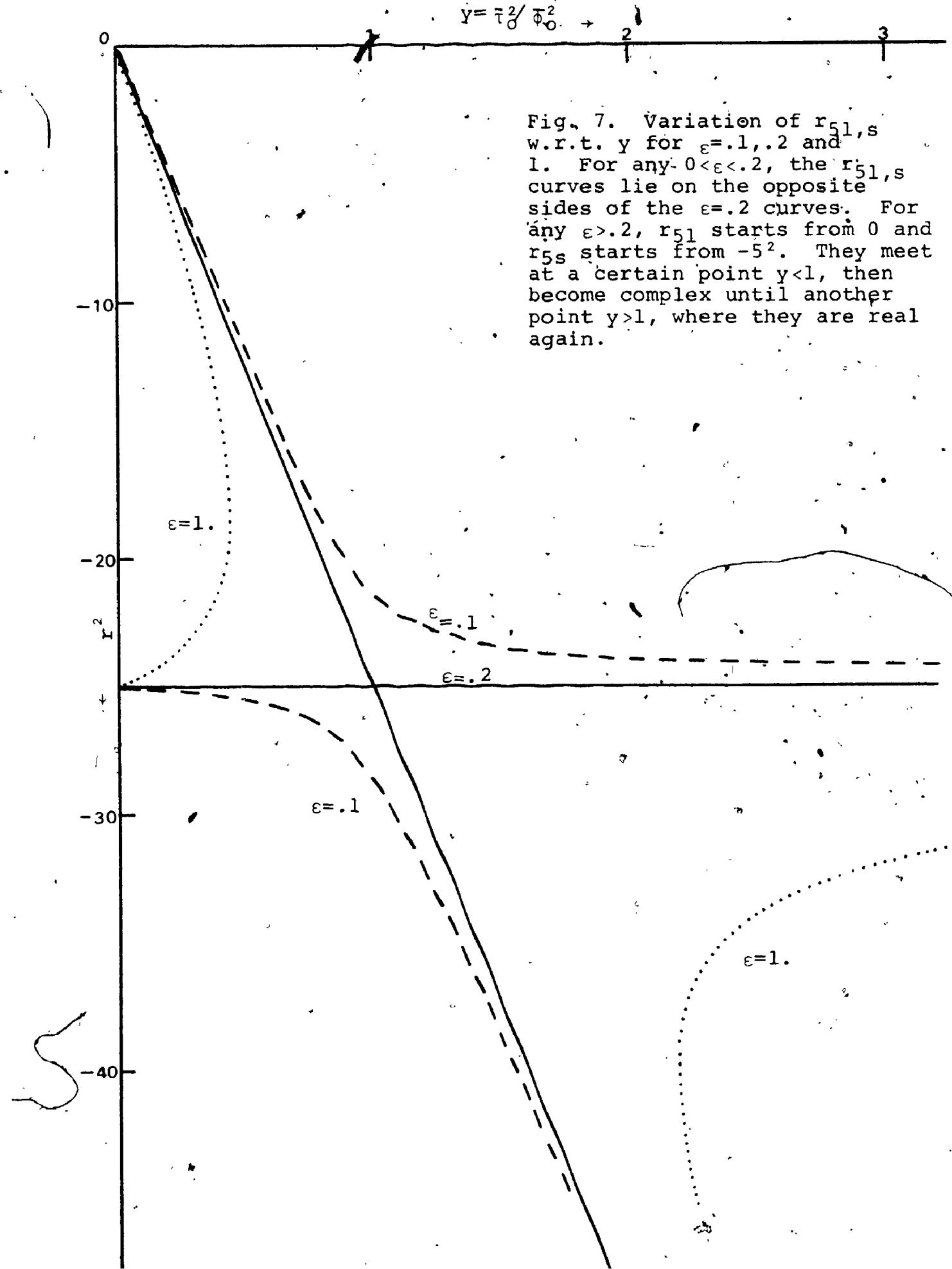

Fig. 7. Variation of $r_{51,s}$ w.r.t. y for ε=.1,.2 and 1. For any $0<\varepsilon<.2$, the $r_{51,s}$ curves lie on the opposite sides of the ε=.2 curves. For any ε>.2, r_{51} starts from 0 and r_{5s} starts from -5^2. They meet at a certain point y<1, then become complex until another point y>1, where they are real again.

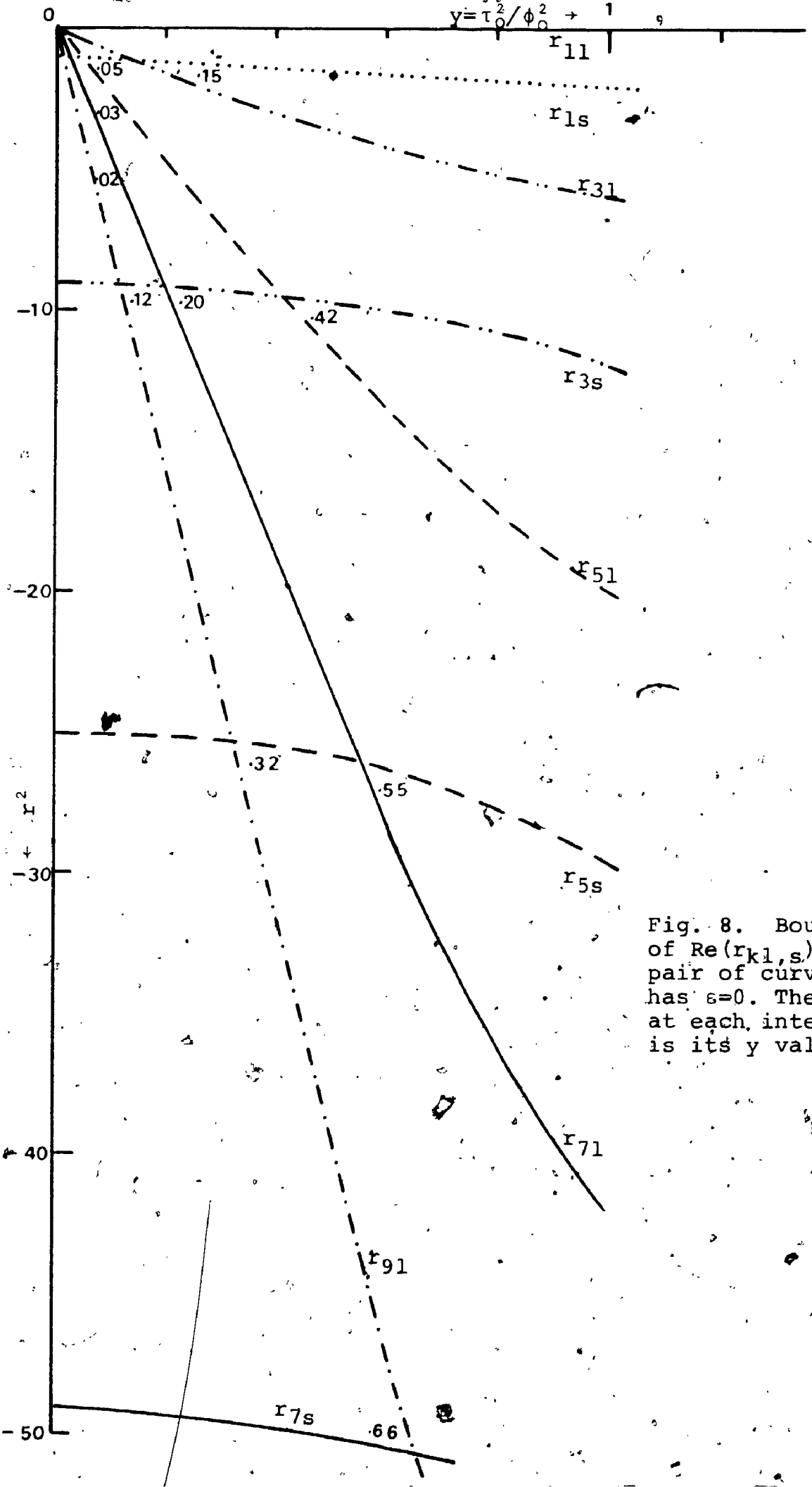

Fig. 8. Boundary of $\mathrm{Re}(r_{k1,s})$. Each pair of curves shown has $\varepsilon=0$. The number at each intersection is its y value.

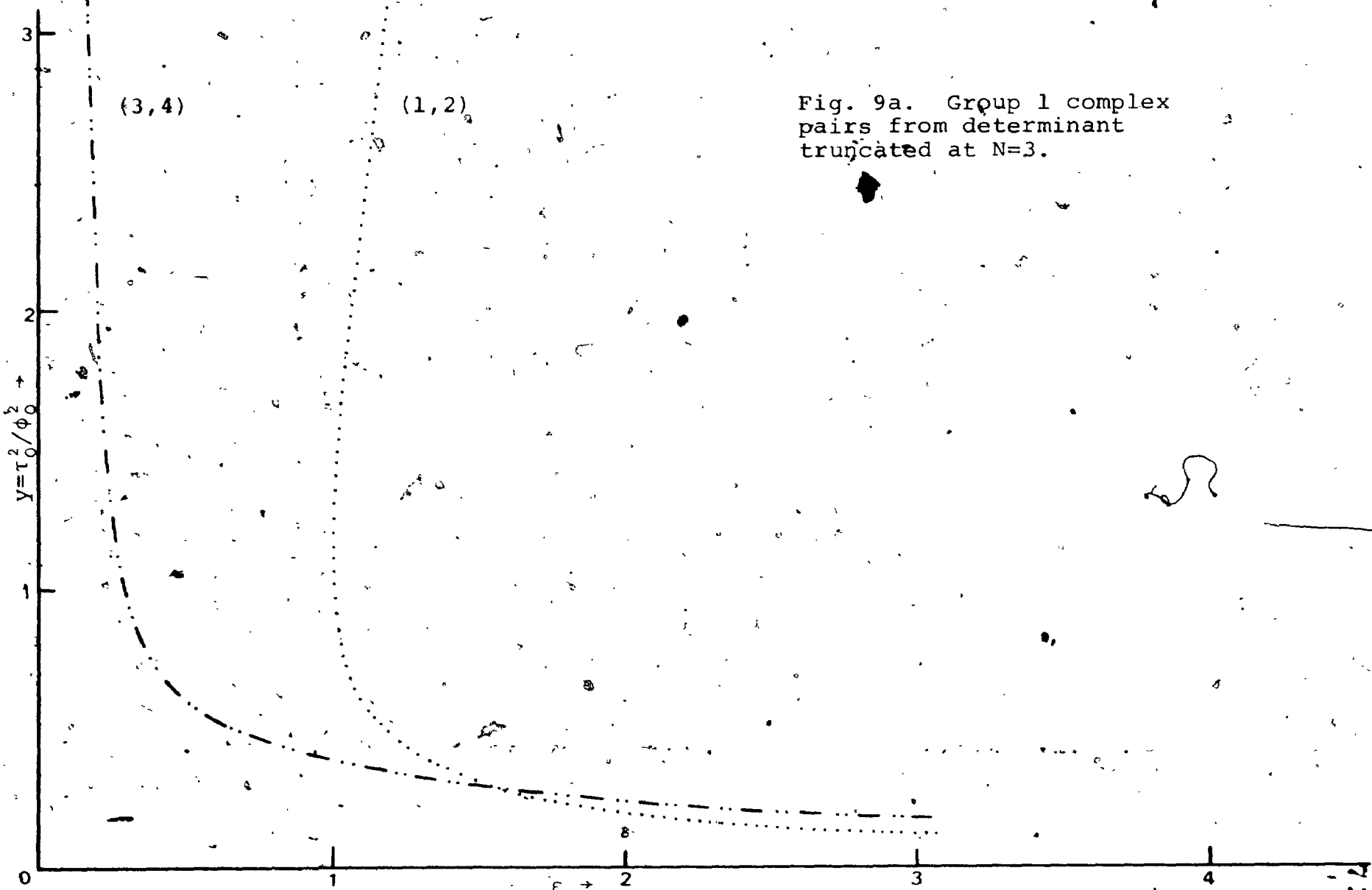

Fig. 9a. Group 1 complex pairs from determinant truncated at N=3.

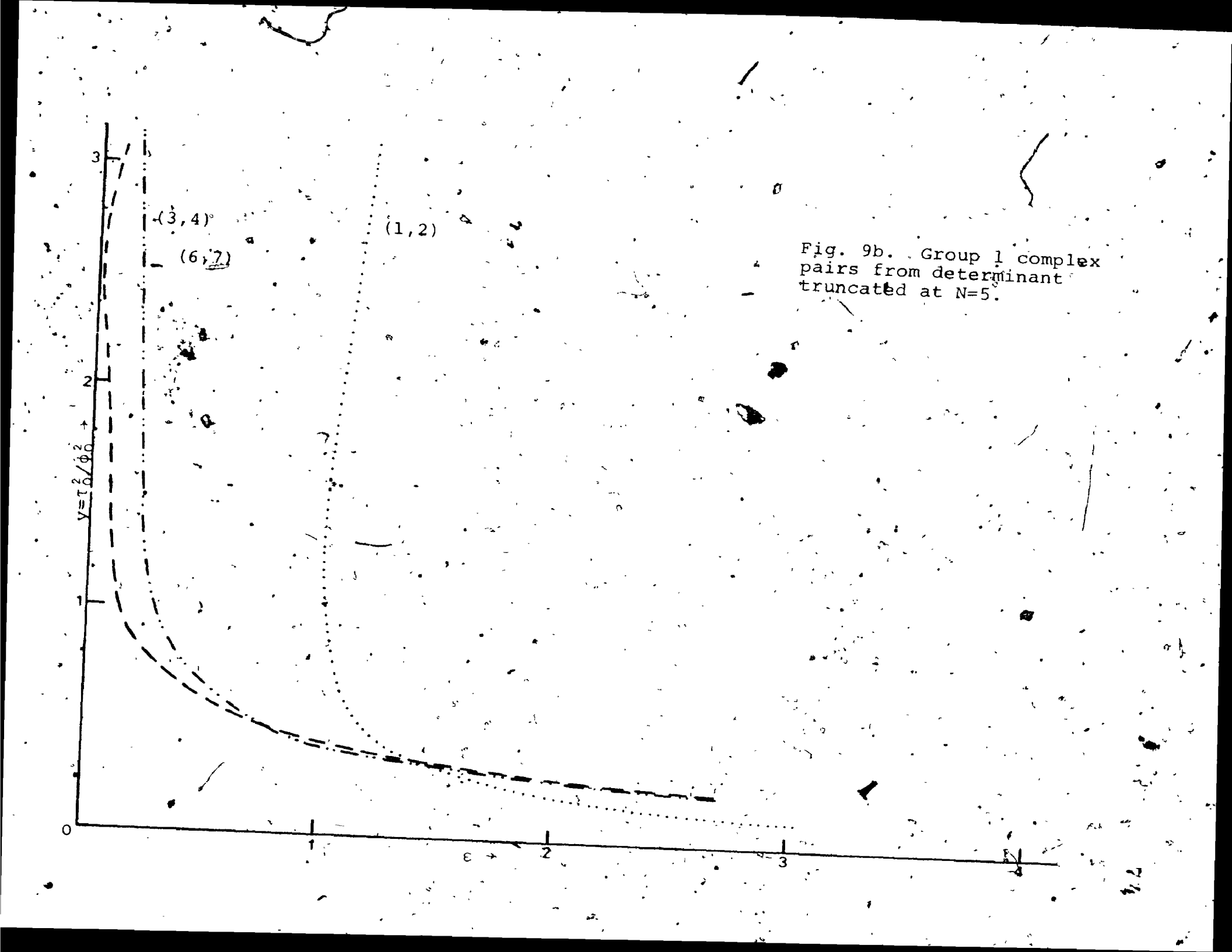

Fig. 9b. Group 1 complex pairs from determinant truncated at N=5.

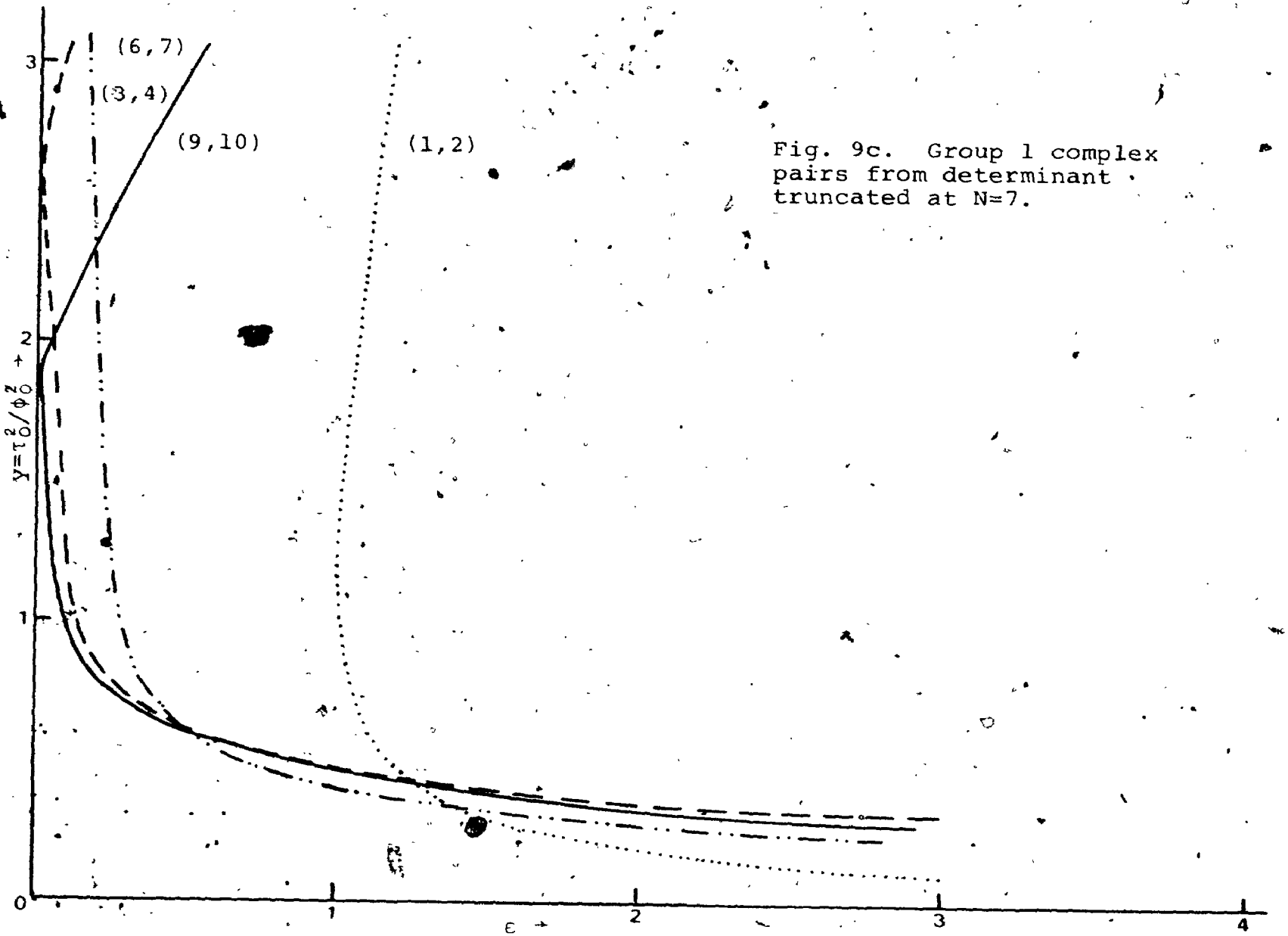

Fig. 9c. Group 1 complex pairs from determinant truncated at N=7.

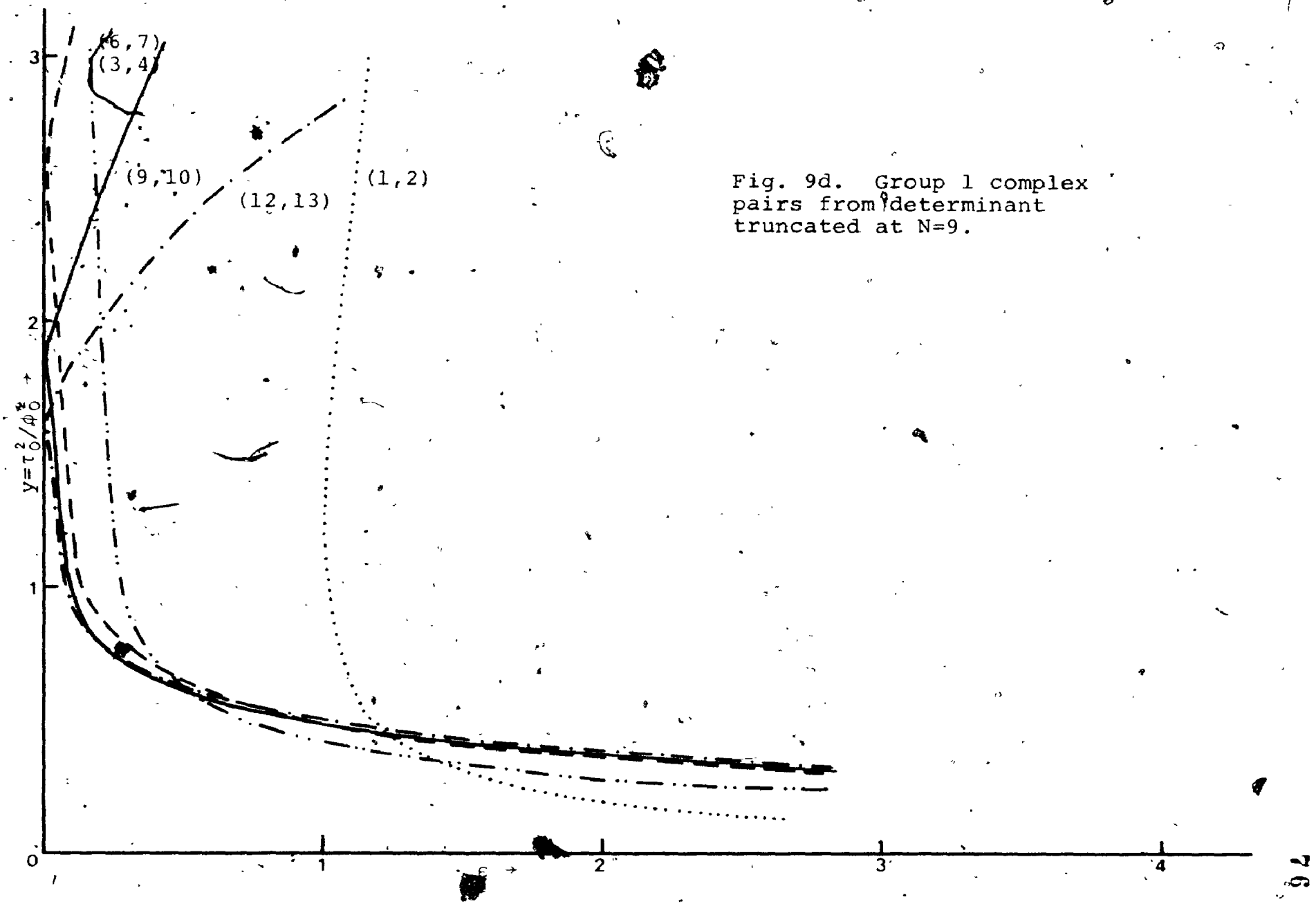

Fig. 9d. Group 1 complex pairs from determinant truncated at N=9.

Fig. 10. Group 2 complex pairs from determinants truncated at N=3,5,7 and 9.

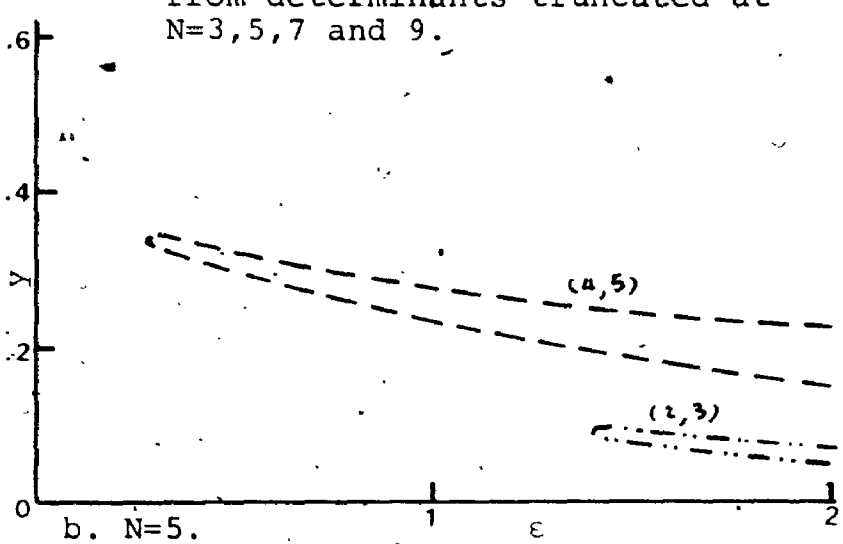

b. N=5.

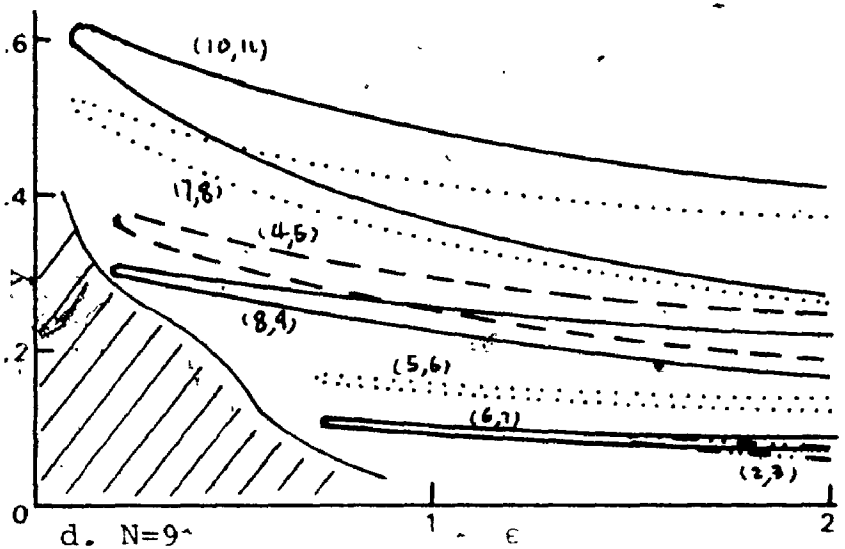

d. N=9

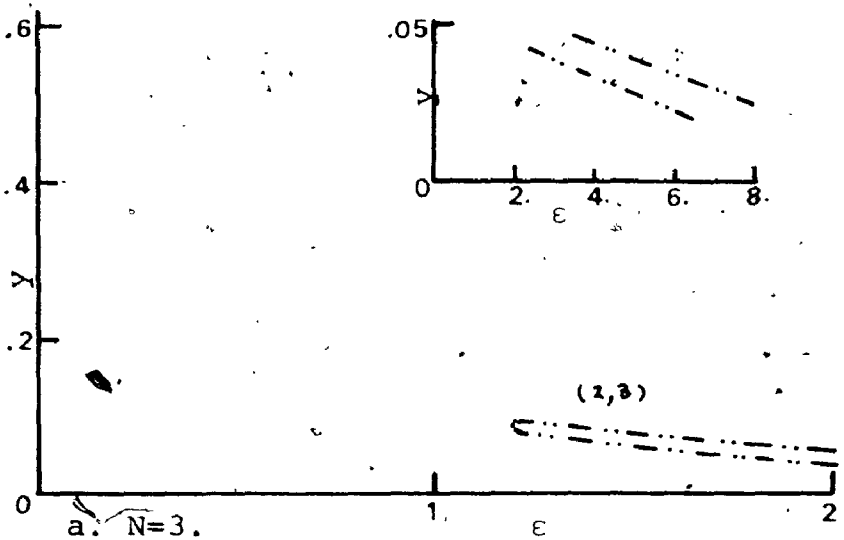

a. N=3.

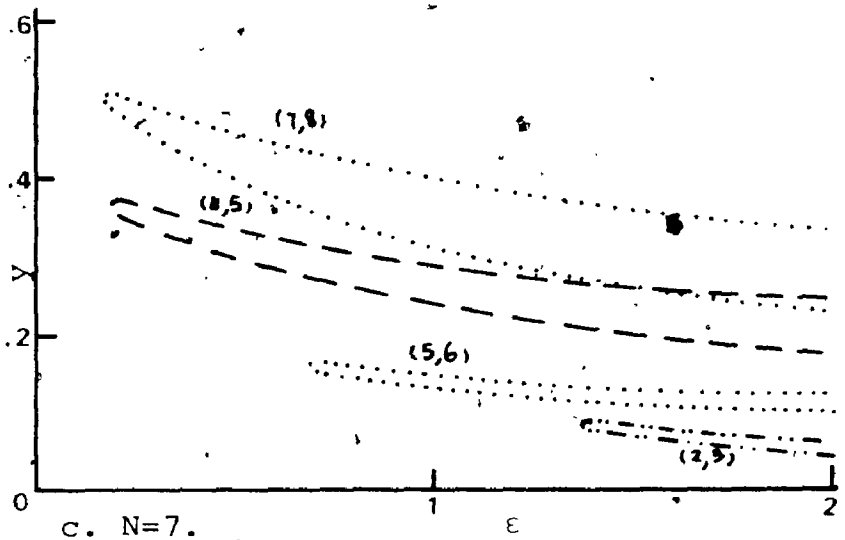

c. N=7.

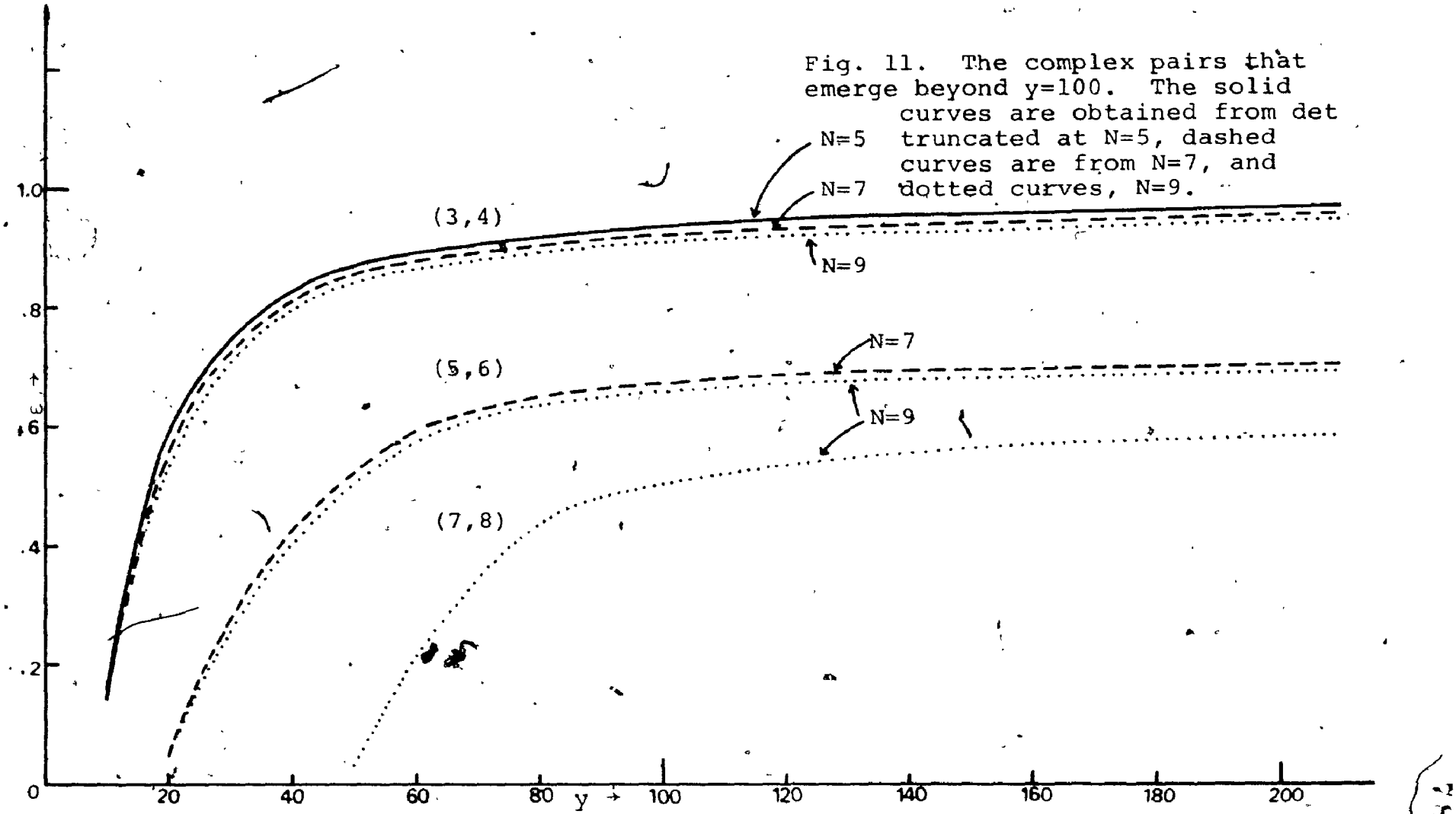

Fig. 11. The complex pairs that emerge beyond y=100. The solid curves are obtained from det truncated at N=5, dashed curves are from N=7, and dotted curves, N=9.

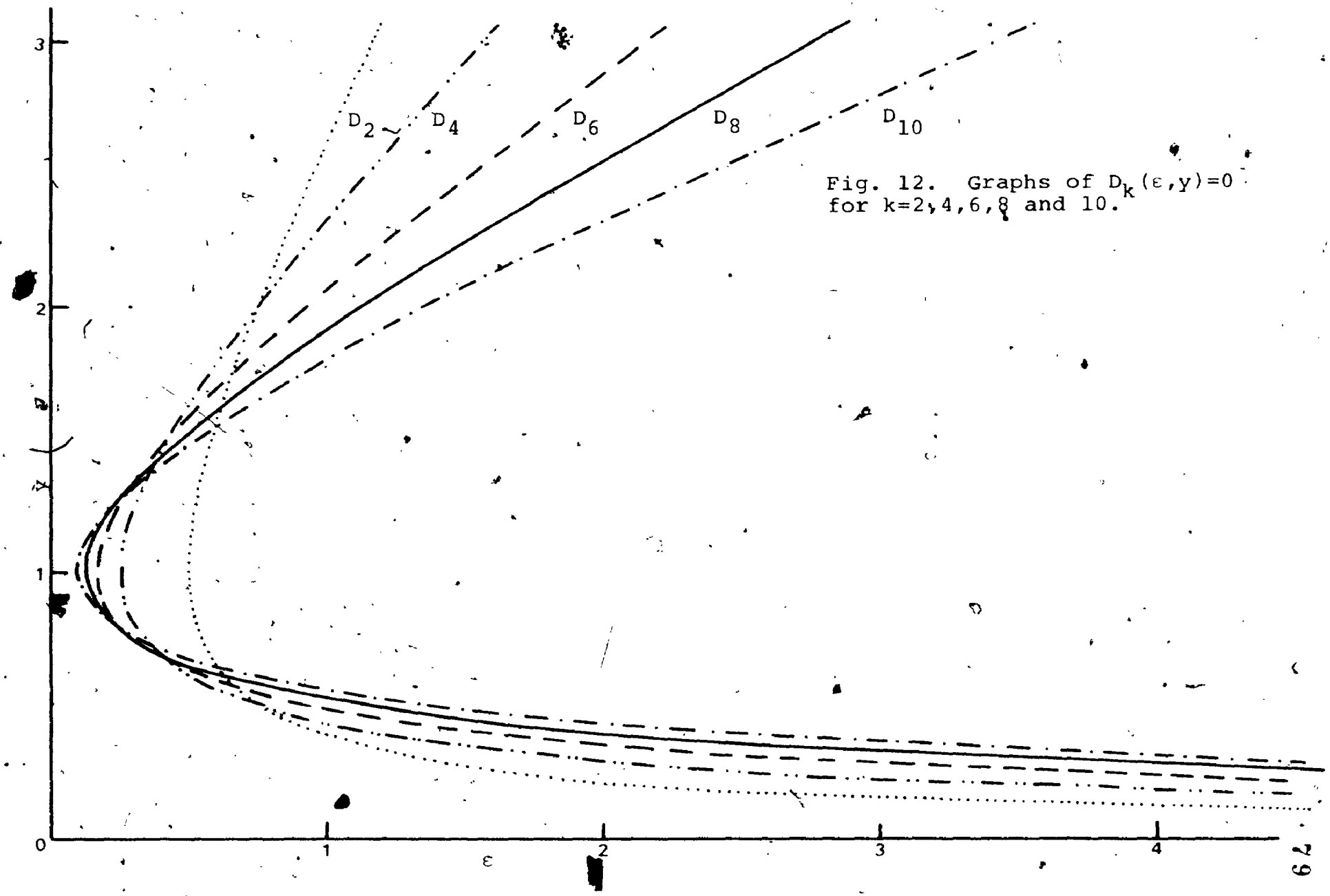

Fig. 12. Graphs of $D_k(\varepsilon,y)=0$ for k=2,4,6,8 and 10.

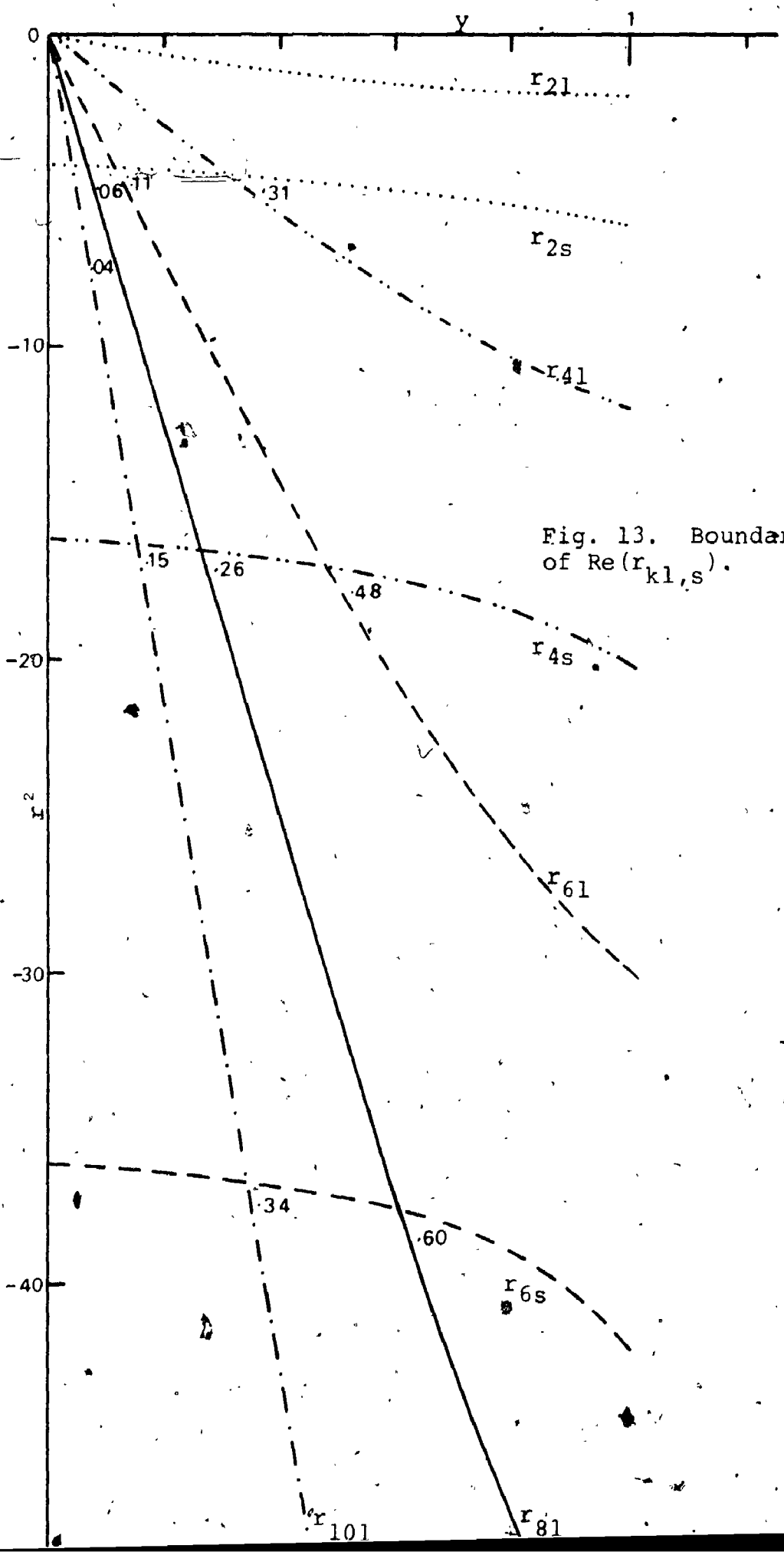

Fig. 13. Boundary of $\mathrm{Re}(r_{k1,s})$.

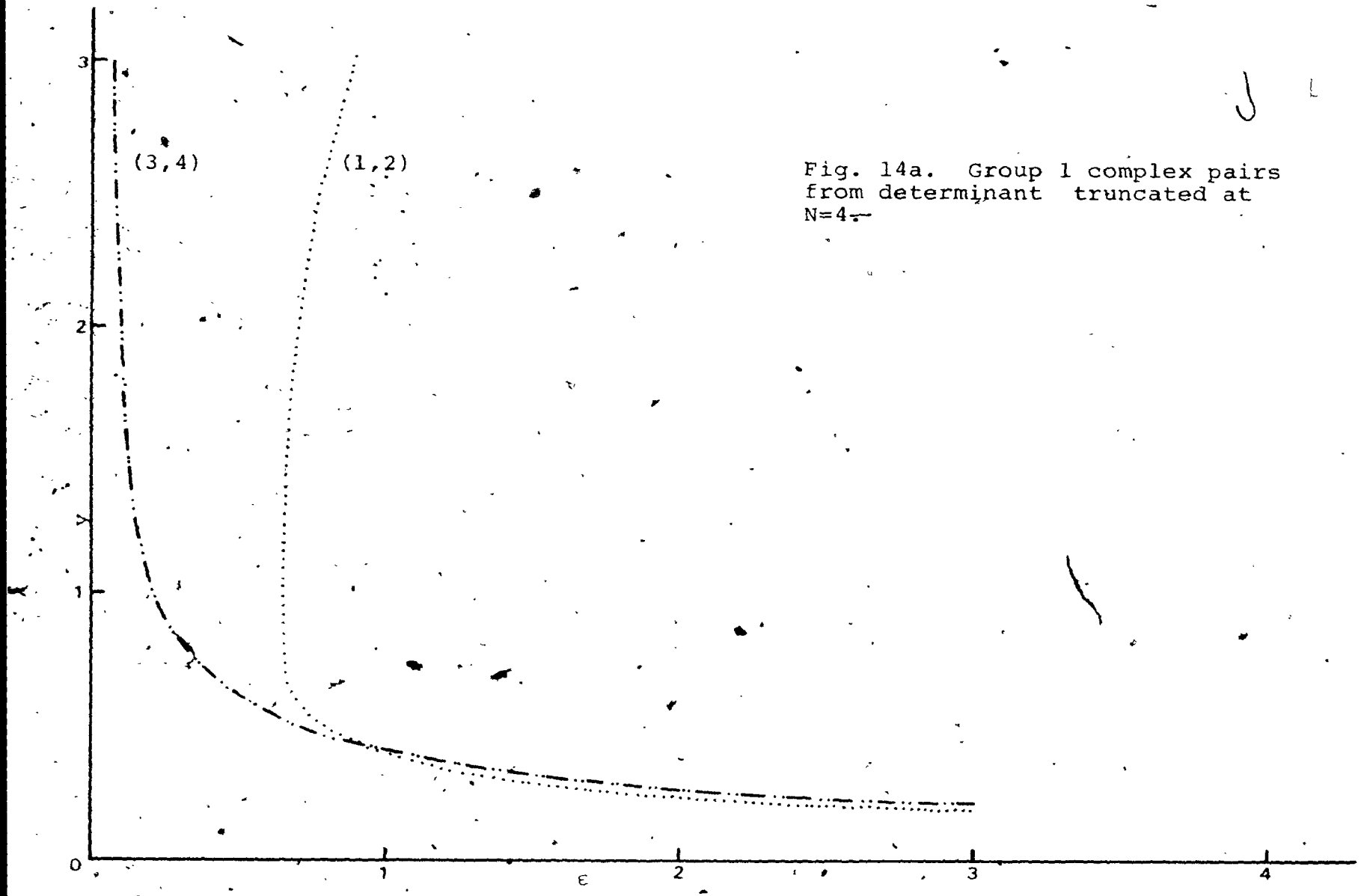

Fig. 14a. Group 1 complex pairs from determinant truncated at N=4.

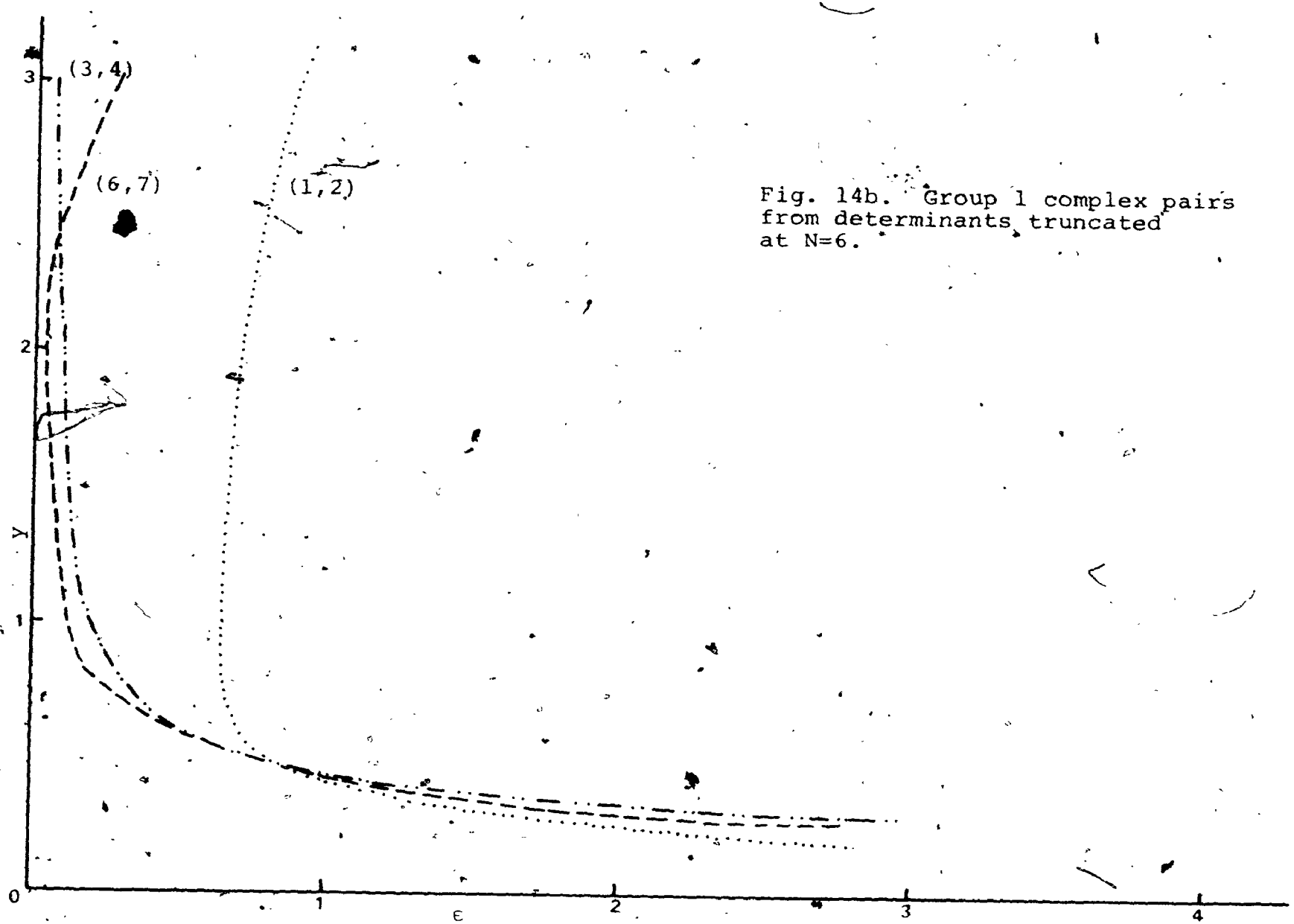

Fig. 14b. Group 1 complex pairs from determinants truncated at N=6.

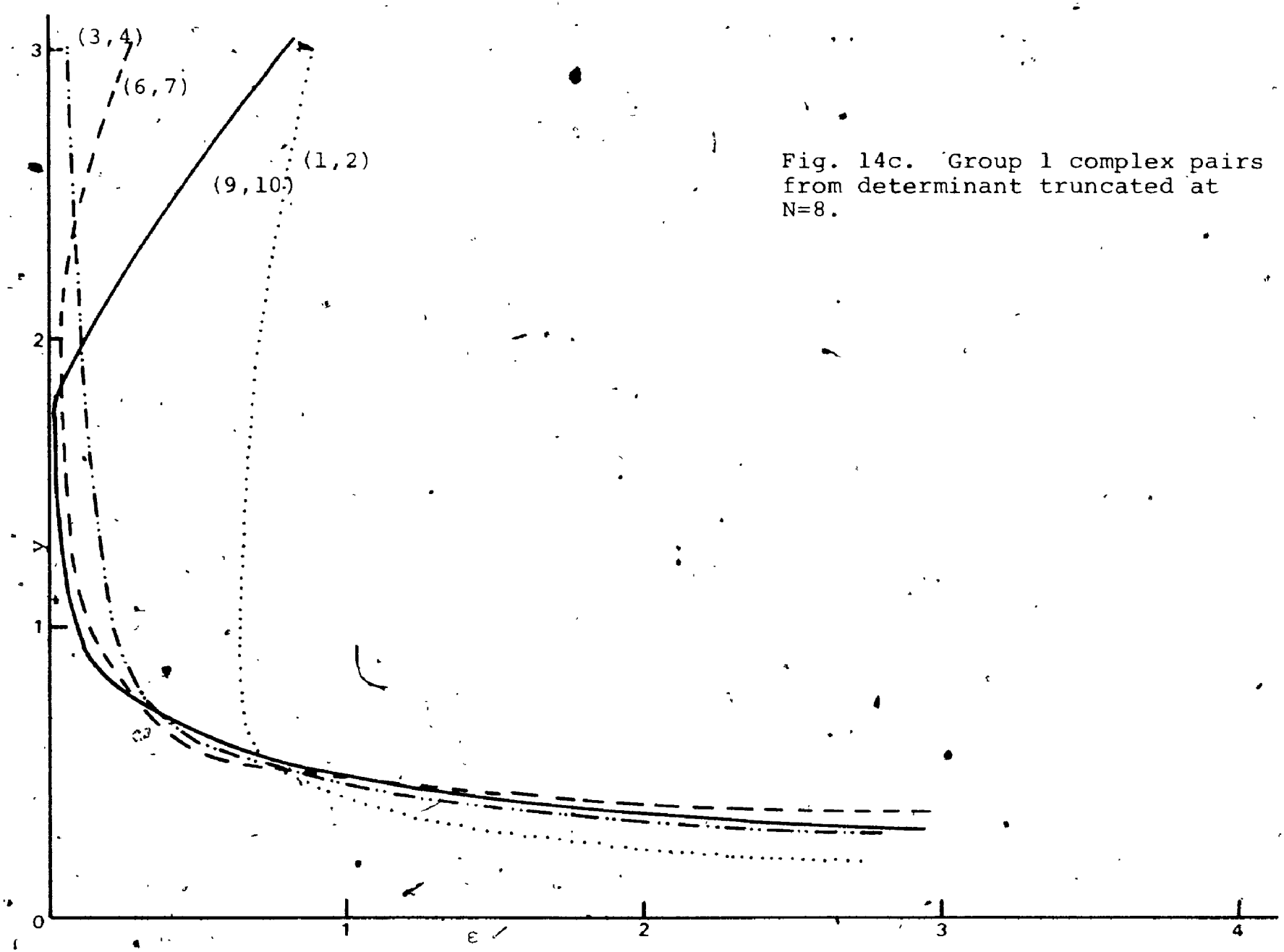

Fig. 14c. Group 1 complex pairs from determinant truncated at N=8.

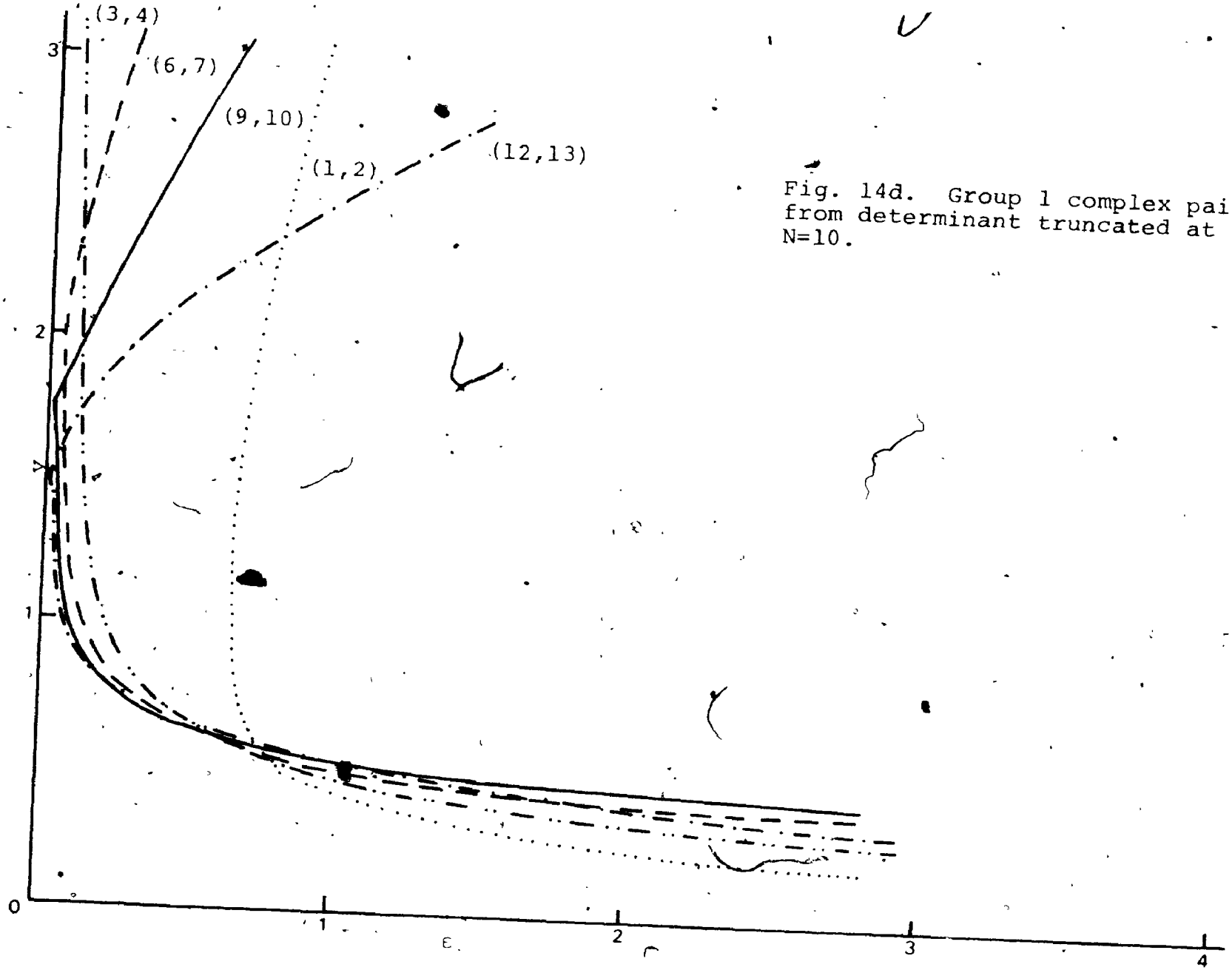

Fig. 14d. Group 1 complex pairs from determinant truncated at N=10.

Fig. 15. Group complex pairs from determinants truncated at N=4,6,8, and 10.

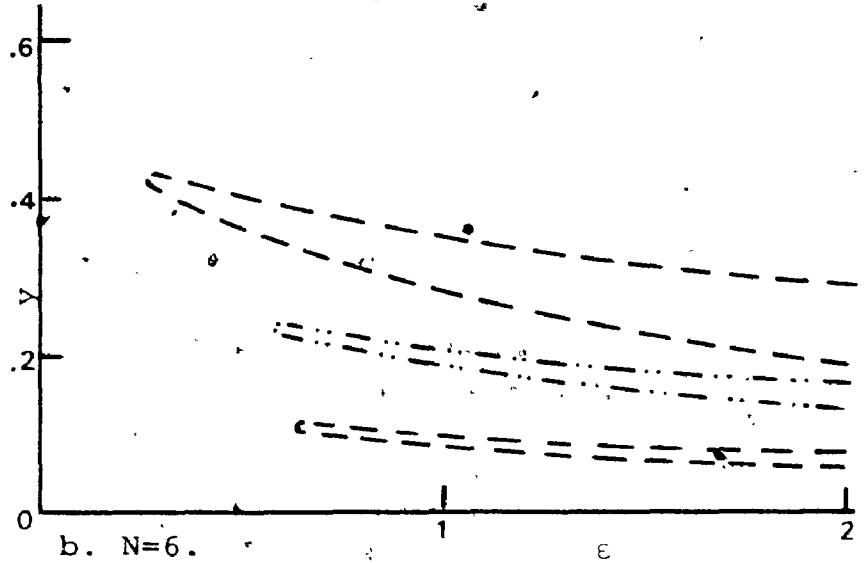

b. N=6.

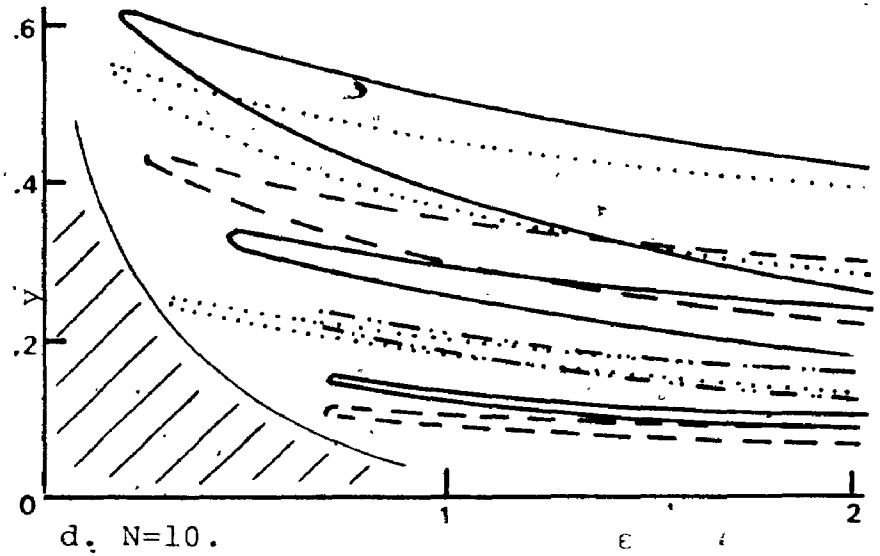

d. N=10.

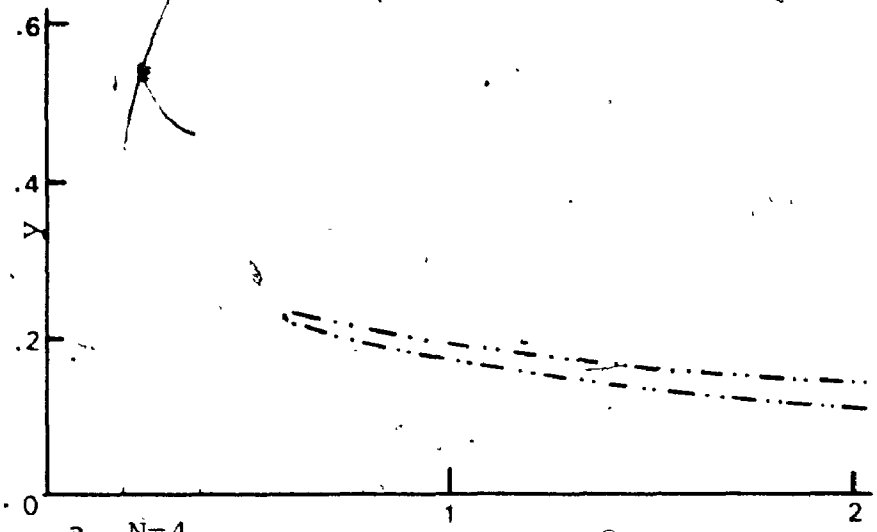

a. N=4.

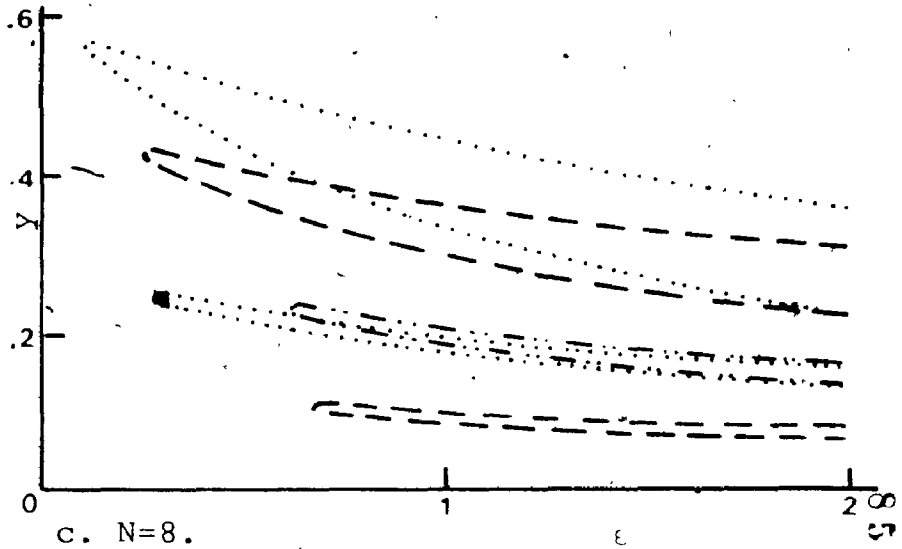

c. N=8.

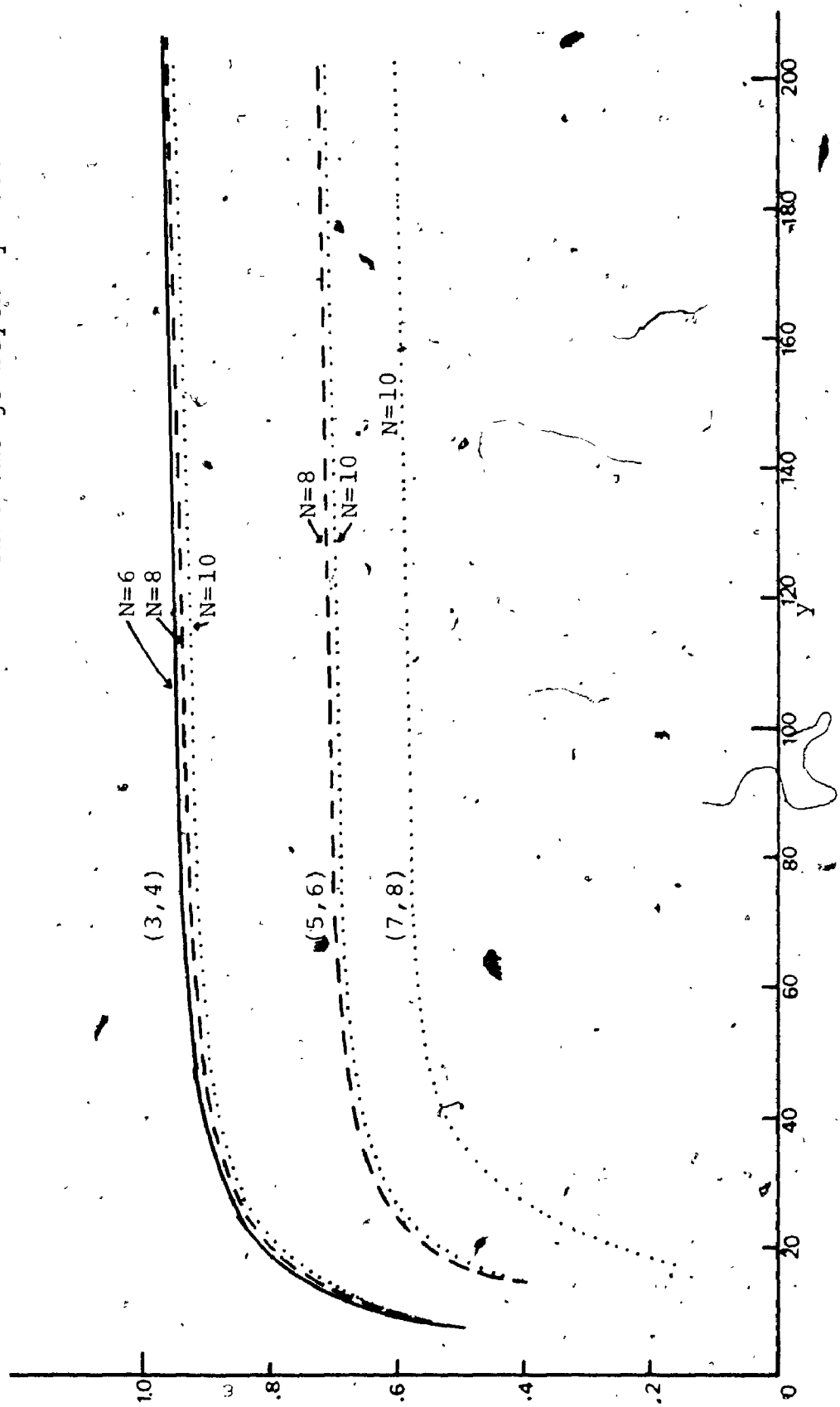

Fig. 16. The complex pairs that emerge beyond y=100.

6. Conclusion.

In this thesis we have studied the stability of some of the zeroth order STS equilibria obtained in reference 27. A mixed Laplace-Fourier method was used to convert the coupled equations (2.7) and (2.8) into a Fredholm integral equation in $\hat{T}(\phi,s)$ given by equations (3.21-28). The complicated kernel (equations (3.25-28)) was reduced to a remarkably simple form of equations (4.25-28). Instead of solving this Fredholm equation we reduced it to systems of linear equations in sine and cosine coefficients of $\hat{T}(\phi,s)$, and obtained a criterion for stability from the zeros of the determinant of the coefficients of the system of linear equations in the cosine coefficients. In the limit when $\varepsilon=0$, the matrix of coefficients is diagonal, and its determinant is easily evaluated. In this simple case we found that our system is stable. For any $\varepsilon>0$, the off diagonal terms are non-zero, and we had to use numerical methods to find the zeros of this determinant. Unlike the $\varepsilon=0$ case, a non-zero ε confines us to the intersection of the hatched corners in fig. 10d and fig. 15d in order to have stability for our system.

If the present method were followed to analyse the stability of the equilibrium solution including the first order term $\beta_2\neq 0$, but $\beta_2^2\to 0$ in reference 27, then trouble develops right after we obtain the position

2 2

OF/DE

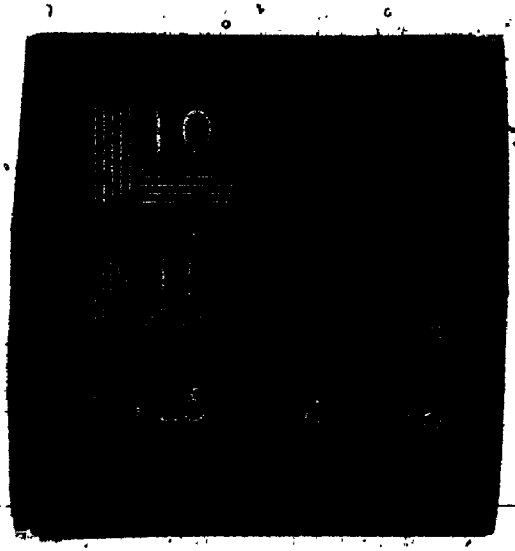

coordinates in terms of ϕ and τ. For after doing the integrations in equations (3.4) and (3.10) we obtain

$$x(\phi) = \pm 1/(1+(1+k_\phi^2)\tan^2\phi/\bar{\tau}_0)^{1/2},$$

$$x(\tau) = x_0 cn(\tau/\bar{\tau}_0, k_\tau),$$

where

$$k_\phi^2 = 4\beta_2,$$

$$k_\tau^2 = 2\beta_2,$$

and cn is the elliptic function. In using these quantities for further integrations in g_n and h_n we encounter with integrals of the form

$$\int_0^{\tau_0} d\tau \frac{e^{in\tau/\bar{\tau}_0} sn(\tau/\bar{\tau}_0) dn(\tau/\bar{\tau}_0)}{x(\phi) + cn(\tau/\bar{\tau}_0)},$$

and

$$\int_0^{\tau_0} d\tau \frac{e^{-in\tau/\bar{\tau}_0}}{x(\phi) + cn(\tau/\tau_0)},$$

both of which are quite impossible to have in closed forms. Even if there exist some method of obtaining a closed closed form for these integrals, we expect them to be as formidable as the usual integrals having elliptic functions in the integrand. This makes the other integration even more difficult.

A thermodynamic approach to this problem is being investigated by Mr. A.B. Tailor at present. His idea is to calculate the entropy S for the electron-ion ring, and obtain a 'yes' or 'no' answer for stability

from the time derivative of S.

As it was mentioned in reference 27, the equilibrium solution has neglected the r dependence which is not permissible in an actual experimental set up, its usefulness is in serving as an input to a numerical program that contains the r dependence as well. Thus there is no point in comparing the present analysis with experimental data which is very crude at present any way.[36] What we have done justifies the use of a water bag model for the class of equilibrium solutions considered, provided no nonlinear effect has set in.

Appendix A

If we take the Laplace transform of (3.5)

$$s\hat{T} + \frac{\partial \hat{T}}{\partial \phi} = T(\phi,0) + e\frac{\partial \hat{\phi}_i^{(1)}(\phi,s)}{\partial \phi}, \qquad (A1)$$

then instead of solving this first order differential equation, we expand $\hat{T}$

$$\hat{T}(\phi,s) = \sum_{k=-\infty}^{\infty} e^{ik\phi/\bar{\phi}_0} T_k(s), \qquad (A2)$$

and obtain the k^{th} component from equation (A1)

$$T_k(s) = \frac{1}{\phi_0(ik/\bar{\phi}_0+s)} \int_0^{\phi_0} d\phi' \left(T(\phi',0) + e\frac{\partial \hat{\phi}_i^{(1)}}{\partial \phi'}\right). \qquad (A3)$$

After going through the same series of substituting as we did in obtaining equations (3.21-28), we get

$$T_k(s) = [\text{inhomogeneous terms}] - \frac{4e^4 C_0}{R^2 z_0^2} \int_0^{\phi_0} d\phi'' \hat{T}(\phi'',s) \frac{1}{2\pi(ik+\bar{\phi}_0 s)} \int_0^{\phi_0} d\phi' e^{-ik\phi'/\bar{\phi}_0} \operatorname{sgn}(\phi') w(\phi') \cdot \int_{H_i^{min}}^{\infty} dH_i \frac{df_i^{(o)}}{dH_i} \sum_{n=-\infty}^{\infty} g_n h_n \qquad (A4)$$

The terms g_n and h_n in the infinite sum are identical to those of equations (3.27) and (3.28), and they can be reduced in the same manner as given in section 4 to

$$-\frac{2z_o n}{(n^2+\bar{\tau}_o^2 s^2)}\,\xi_n(\phi',\phi'').$$

The H_i integration runs into similar difficulty as in section 4, and it can be resolved by the same argument given there. The ϕ integration differs from the main test in that there the exponential factor had $s\phi$ as its argument, whereas here, we have $-ik\phi/\bar{\phi}_o$. This difference has the effect of picking up only those terms that contain a factor $\sin k\phi/\bar{\phi}_o/\sin\phi/\bar{\phi}_o$ from the infinite sum, by the following integral

$$\int_0^{\phi_o} d\phi\; e^{-ik\phi/\bar{\phi}_o}\sin n\phi/\bar{\phi}_o = -\frac{i\phi_o}{2}\delta_{kn} \qquad (A5)$$

where δ_{kn} is the Kronecker delta. Bearing this in mind, and for k=odd=2p+1, equation (A4) can be reduced to

$$T_{2p+1}=[\text{inhomo}] - \frac{i}{i(2p+1)+\bar{\phi}_o s}\Big[\frac{(2p+1)^2\varepsilon p-1}{u_{2p+1}}\sum_{i=0} C_{2i+1} + \frac{(2p+1)((2p+1)\varepsilon-1)}{u_{2p+1}}C_{2p+1} + (2p+1)\sum_{i=p+1}^{\infty}\frac{2i+1}{u_{2i+1}}C_{2i+1}\Big]. \qquad (A6)$$

A similar equation can be developed for $k=-(2p+1)<0$

$$T_{-(2p+1)}=[\text{inhomo}] + \frac{i}{-i(2p+1)+\phi_o s}\Big[\frac{(2p+1)^2\varepsilon p-1}{u_{2p+1}}\sum_{i=0} C_{2i+1} + \frac{(2p+1)((2p+1)\varepsilon-1)}{u_{2p+1}}C_{2p+1} + (2p+1)\sum_{i=p+1}^{\infty}\frac{2i+1}{u_{2i+1}}C_{2i+1}\Big], \qquad (A7)$$

where the difference in sign from those of (A6) arises from the exponential factor of equation (A5). The lhs of these two equations are related to C_{2p+1} by

$$C_{2p+1} = \frac{T_{(2p+1)} + T_{-(2p+1)}}{2}.$$

Substituting the rhs of equations (A6) and (A7) into the above we get

$$C_{2p+1} = [\text{inhomo}] + \frac{(2p+1)^3\varepsilon}{u_{2p+1}v_{2p+1}} \sum_{i=0}^{p-1} C_{2i+1}$$
$$+ \frac{(2p+1)^2((2p+1)\varepsilon-1)}{u_{2p+1}v_{2p+1}} C_{2p+1} + \frac{(2p+1)^2\varepsilon}{v_{2p+1}} \sum_{i=p+1}^{\infty} \frac{(2i+1)}{u_{2i+1}} C_{2i+1}], \quad \text{(A8)}$$

which is just the (2p+1)th row of equation (5.6). Hence the equivalence of the two methods is proven.

Appendix B

All the identities used in this appendix are taken from section (10.11) of Higher Transcendental Functions by the Staff of Bateman Manuscript Project.[33] Since the enumeration of equations used there are Arabic numerals, we shall quote them without adding the phrase 'of Bateman Manuscript'. There is no confusion with those equations from reference 27 either, because we will not be using any of them in this appendix. In order to save some time in typing we do not include the arguments of the Tchebycheff polynomials, since they all have the same argument $x=-x'/x_o$, for the derivation of $xU'_{n-1}(x)$; and $x=-x''/x_o$ for the derivation of $xT'_n(x)$.

From the derivative formula (21) we get

$$xU'_{n-1} = \frac{x[nU_{n-2} - (n-1)xU_{n-1}]}{1 - x^2},$$

$$= [\frac{nxU_{n-2} - (n-1)U_{n-1}}{1 - x^2}] + (n-1)U_{n-1}. \quad (B1)$$

Our task now is to transform the square bracket into a linear combination of the U_n's. It turns out that there are two forms of linear combination depending on whether n is odd or even.

For an even indexed U, say U_{2p}, equation (40) gives

$$U_{2p} = 2\left(\sum_{m=1}^{p} T_{2m} + 1/2\right), \quad p>0,$$

and T_{2m} can be obtained from equation (41)

$$T_{2m} = 1 - 2(1-x^2)\sum_{i=0}^{m-1} U_{2i}, \quad m>0,$$

which means

$$U_{2p} = \left((2p+1) - 4(1-x^2)\sum_{m=1}^{p}\sum_{i=0}^{m-1} U_{2i}\right), \quad p>0,$$

$$= \left((2p+1) - 4(1-x^2)\sum_{i=0}^{p-1}(p-i)U_{2i}\right), \quad p>0.$$

Similarly, using equation (40) and (42), the odd indexed U_{2p-1} can be expressed as

$$U_{2p-1} = 2\sum_{m=1}^{p-1} T_{2m+1} + 2x, \quad p>1$$

$$= 2px - 4(1-x^2)\sum_{m=1}^{p-1}\sum_{i=0}^{m-1} U_{2i+1}, \quad p>1$$

$$= 2px - 4(1-x^2)\sum_{i=1}^{p-1}(p-i)U_{2i-1}, \quad p>1.$$

If we accept the convention that whenever the upper limit of a summation is less than the lower limit then the sum is zero, that is

$$\sum_{i=j}^{k} g_i = 0, \text{ if } k<j, \tag{B2}$$

Then the restriction on p in U_{2p} and U_{2p-1} can be extended

$$U_{2p} = (2p+1) - 4(1-x^2)\sum_{i=0}^{p-1}(p-i)U_{2i}, \quad p\geq 0, \tag{B3}$$

$$U_{2p-1} = 2px - 4(1-x^2)\sum_{i=1}^{p-1}(p-i)U_{2i-1}, \quad p\geq 1. \tag{B4}$$

These two equations can be used to consider the odd and even cases of (B1). For n=odd=2p+1, the square bracket of (B1) become

$$\begin{aligned}&((2p+1)xU_{2p-1} - 2pU_{2p})/(1-x^2)\\ &=4[2p\sum_{i=0}^{p-1}(p-i)U_{2i}-(2p+1)x\sum_{i=1}^{p-1}(p-i)U_{2i-1}]\\ &\quad - 2p(2p+1).\end{aligned} \tag{B5}$$

If we recognize $x=T_1$, then the second term can be expressed as a sum of the U_n's by equation (36)

$$\begin{aligned}xU_{2i-1} &= T_1U_{2i-1},\\ &= (U_{2i} + U_{2i-2})/2.\end{aligned}$$

Substituting this into the square bracket of (B5), we get

$$\begin{aligned}&2p\sum_{i=0}^{p-1}(p-i)U_{2i}-(2p+1)x\sum_{i=1}^{p-1}(p-i)U_{2i-1}\\ &\quad = 2p\sum_{i=0}^{p-1}(p-i)U_{2i}-(2p+1)\sum_{i=1}^{p-1}(p-i)(U_{2i}+U_{2i-2})/2,\end{aligned}$$

$$= 2p \sum_{i=0}^{p-1} (p-i)U_{2i} - (2p+1) \sum_{i=1}^{p-i} \frac{p-i}{2} U_{2i}$$

$$- (2p+1) \sum_{i=0}^{p-2} \frac{(p-i-1)}{2} U_{2i},$$

$$= (p^2 + \frac{p+1}{2})U_o + \sum_{i=1}^{p-1} \frac{2i+1}{2} U_{2i}, \qquad p>1,$$

where the second line was obtained by putting i=i-1, and the third line was straightforward collecting like terms. Substituting this into (B5) we obtain

$$\frac{(2p+1)xU_{2p-1} - 2pU_{2p}}{1 - x^2} = 4 \sum_{i=0}^{p-1} \frac{2i+1}{2} U_{2i}, \quad p \geq 1,$$

where p=1 was obtained by direct verification. Thus xU'_{n-1}, for n=2p+1, can be expressed as a linear combination of the U's

$$xU'_{2p} = 4 \sum_{i=0}^{p-1} (i+1/2)U_{2i} + 2pU_{2p}, \qquad \text{(B6)}$$

and this is valid for $p \geq 0$. Since the derivation for the even case is exactly similar, we just quote the result for n=even=2p+2

$$xU'_{2p+1} = 4 \sum_{i=0}^{p-1} (i+I)U_{2i+1} + (2p+1)U_{2p+1}, \quad p \geq 0.$$

(B7)

From the derivative formula (20) we get

$$xT_n' = \frac{nx(T_{n-1} - xT_n)}{1 - x^2},$$

$$= \frac{nxT_{n-1} - nT_n}{1 - x^2} + nT_n,$$

by equation (4) the first term is just nU_{n-2}, therefore

$$xT_n' = nU_{n-2} + nT_n. \tag{B8}$$

We find it useful for the final results if U_{n-2} were expressed in terms of T's only. From equation (40) for $n=2p+1$, $n-2=2p-1$,

$$U_{2p-1} = 2\sum_{i=0}^{p-1} T_{2i+1}.$$

Hence (B8) reduces to a linear sum of the T's

$$xT'_{2p+1} = 2(2p+1)\sum_{i=0}^{p-1} T_{2i+1} + (2p+1)T_{2p+1}. \tag{B9}$$

For n=even=2p+2,

$$xT'_{2p+2} = 2(2p+2)\left[\sum_{i=0}^{p} T_{2i} - 1/2\right] + (2p+2)T_{2p+2}. \tag{B10}$$

References:

1. G.I. Budker; Proc. CERN Symposium on High Energy Accelerators, 68, (1956).

2. R.B. R-S-Harvie; AERE memorandum G/M87, (1951).

3. H. Alfven and P. Werholm; Arkiv Fysik, 5, 175, (1952).

4. I.J. Billington and W.R. Randorf; Wireless Engineer, 31, 287, (1954).

5. V.I. Veksler; Proc. CERN Symposium on High Energy Accelerators, 80, (1956).

6. M.L. Levin, G.A. Askaryan, and M.S. Rabinovich; Proc. CERN Symposium on High Energy Accelerators, (1959).

7. G.A. Askaryan, M.L. Levin, M.L. Jovnovich, and M.S. Rabinovich; Conference on Plasma Physics and CTR, Salzburg, (1961).

8. D.C. dePackh; Third International Conference on Ionization Phenomena in Gases, Venice, 236, (1957).

9. D.C. dePackh; Journal of Electronics and Control, 13, 417, (1962).

10. T.F. Godlove and D.C. dePakch; Journal of Applied Physics, 31, 2016, (1960).

11. J.B. Ehrman; Physics of Fluids, 3, 121, (1960).

12. J.B. Ehrman; ibid., 3, 303, (1960).

13. J.B. Ehrman; Plasma Physics, 8, 377, (1966).

14. V.I. Veksler; Cambridge Electron Accelerator Report No. CEAL-2000, 289, (1967).

15. D. Keefe, G.K. Lambertson, L.J. Laslett, W.A. Perkins, J.M. Peterson, A.M. Sessler, R.W. Allison, W.W. Chupp, A.U. Luccio, and J.B. Rechen; Physics Review Letters, 22, 558, (1969).

16. W.B. Lewis; Symposium on ERA, LRL Report, No. UCRL-18103, 6, (1968).

17. R.E. Berg, H. Kim, M.P. Reiser, and G.T. Zorn; Physics Review Letters, 22, 419, (1969).

18. L.J. Laslett and A.M. Sessler; IEEE Transaction on Nuclear Science, NS-16, No. 1, 1034, (1969).

19. P.C. Clemmow and J.P. Dougherty; Electrodynamics of Particles and Plasma, Chapter 11.

20. D.C. dePackh; Proposal for Electron Ring Accelerator Studies, N.R.L., Washington, D.C., May, (1969).

21. J.K. Burton, J.J. Condon, W.H. Lupton, F.L. Desrosier, A.C. Greenwald, J.M. Henness, M.J. Rhee, and G.T. Zorn; IEEE, Transactions on Nuclear Science, NS-20, No. 3, 321, (1973).

22. J.G. Kalnins, H. Kim, and D.L. Nelson; IEEE, Transaction on Nuclear Science, NS-18, No. 3, 473, (1971).

23. C.D. Striffler, C.A. Kapetanakos, and R.C. Davidson; Paper 2B10, 1st International IEEE Conference on Plasma Science, May, (1974).

24. E. Ott and R.N. Sudan; Physics of Fluids, 14, 1831, (1971).

25. E. Ott; Plasma Physics, 13, 529, (1971).

26. R.C. Davidson and J.D. Lawson; Particle Accelerator, 4, 1, (1972).

27. J.B. Ehrman; Filament Model for a Stationary Field Electron Ring Accelerator: The Generalized Bernstein-Green-Kruskal Problem, to be published in Journal of Plasma Physics, (1974).

28. D. Keefe; Particle Accelerators, 1, 1, (1970).

29. W.H. Kegel; Plasma Physics, 12, 105, (1970).

30. G. Schmidt; Physics Review Letters, 26, 952, (1971).

31. W.H. Bennett; Physical Review, 45, 890, (1934).

32. R.C. Davidson; Methods in Nonlinear Plasma Theory, Section 3.5.2. (Academic Press)

33. Staff of the Bateman Manuscript Project; Higher Transcendental Functions, Vol. 2, Section 10.11. (McGraw-Hill)

34. S.G. Mikhlin; Integral Equations, Chapters 1 & 2. (MacMillan Co.)

35. M. Bôcher and L. Brand; Ann. of Math., 13, 167, (1911).

36. Section E, Proc. of the 1973 Particle Accelerator Conference; IEEE Transaction on Nuclear Science, NS-20, No. 3, (1973).